Development of Absorbents for Removal of Pollutants from Hydrosphere

（水圏からの汚染物質除去のための吸着材料の開発）

北海道大学　大学院国際食資源学院

国際食資源学専攻　博士後期課程

Hokkaido University Graduate School of Global Food Resources

Shuang Li

Table of Contents

Title: Development of Absorbent Absorption Kinetic for Removal of Pollutants from Hydrosphere

Chater 1

Introduction

Chapter 1

Introduction

1.1 Pollution in hydrosphere

The presence of water pollutants has always been a significant environmental problem. One of the problems that mankind has been trying to eliminate and figure out. Pollutants have been occurred by natural disasters and anthropogenic factors. Human activity has been reported that could cause the most long-term pollutants accumulation in the hydrosphere [1-2]. The most common water pollutants are coming from various approaches, like nuclear leakage pollution in seawater and freshwater, heavy metal and organic compounds contaminated in freshwater [3-5]. These toxic pollutants are severe threats to the health of humans and marine life through the daily diet. In fact, the sources of water pollution have always been controversial in water treatment science [6]. Many researchers believe that there are various kinds of radioactive substances and heavy metal ions in nature itself, which cause the contamination of water resources with the change of climate and long-term accumulation [7-9]. Most of the studies also reported that the pollution of water resources are mainly caused by kinds of anthropologic activities, such as the development of urbanization and industrialization damage to water, greywater without treatment of sewage discharge in almost developing countries, moreover, coal mining causes the drinking pollution of heavy metals, as well as the continuous occurrence of nuclear power plants accident and nuclear weapons explosion leakage in recent years, resulting in the pollution of a variety of long-lived radioactive

substances accumulation in water bodies [10-12]. There is a prediction of the World Health Organisation (WHO), approximately 50% of the population will face a water crisis in all of the world by 2025 as well. Thus, facing these phenomena, the biggest challenge is how to improve the water treatment methods and achieve discharged water resource reutilization.

1.1.1 Radioactive substances in hydrosphere

With the development of the world economy, many countries have devoted themselves to building nuclear power plants [13-14]. Since World War II, nuclear substance leakage has been one of the constant water issues due to the nuclear power plant explosion accidents. Regarding the IAEA (International Nuclear Event Scale), there are two major accidents of radioactive substances contamination leakage issues [15]. One is the Chernobyl disaster that occurred at the Chernobyl Nuclear Power Plant in 1986, Soviet Union, which destroyed the city of Pripyat and nearby coastline, and killed up to two hundred thousand people in total by 2004 [16]. Until now, a high concentration of radioactive substances could be detected in the local soil and drinking water. Fish and other marine life are not available to be uptake from that area [17]. Another big one nuclear leakage accident has occurred at the Fukushima Nuclear Power Plant in 2011, Japan, which had been confirmed that radioactive effluent from Fukushima Accident is leaking into the Pacific Ocean even emergency water treatments were conducted [17]. High concentrations of ^{136}Cs, ^{133}I, ^{90}Sr, ^{89}Sr ^{129}I, and U isotopes contaminated nearby coastal harbor. These nuclear power plant accidents generated

several radionuclides such as ^{90}Sr, ^{129}I, and ^{134}Cs are long-lived β-emitter radionuclides, which are undegradable into the organism, readily caused a hazard to the fishery and health of humans [18-19]. Therefore, it is necessary to remove those long-lived radionuclides from water resources as soon as possible.

1.1.2 Heavy metals in hydrosphere

Besides radionuclides leakage, heavy metal contamination is also an important substance as water pollutants. Pollutants of heavy metal are copper, chromium, cadmium, lead in water resources [20-21]. These heavy metal ions are highly toxic, non-biodegradable, easy to accumulate in human organs causing various diseases and health disorders [22]. There are a lot of reports of heavy metal toxicity through drinking water, for example, in early Japan cadmium poisoning led to humans bone softening, kidney failure, resulting in ITAI-ITAI disease, which is named from people make an Itai sound when they are in pain [23-24]. Regarding WHO reports, every year approximately 83,000 population died from diarrhoea due to drinking toxic substances contaminated water, and unsafe sanitation [25]. In addition, due to the continuous issue of heavy metal pollution in water resources, WHO has set the standard level of various heavy metals in drinking water, copper should be less than 2 mg/L, 0.05 mg/L for chromium, 0.003 mg/L for cadmium, and 0.01 mg/L for lead [26]. In order to meet the standards level set by the WHO, water treatment technology is requested for constant improvement, as pollution has continued to be grievous, moreover, water treatment technologies also need to be implemented to resue discharged water and protect the

drinking water from pollution.

1.1.3 Arsenic pollutants in hydrosphere

Arsenic has properties of both metallic and non-metallic elements, which is the most abundant element in the natural environment [27]. Moreover, arsenic is one of the most toxic elements that threaten human health because of its non-degradability [28]. It is easy to transfer to humans through drinking water and a daily diet. Arsenic oxidation states are commonly found in drinking water in the pentavalent state and trivalent state [29]. High concentrations of arsenic can be found in groundwater in many countries, particularly released in America, China, Australia, India, and Bangladesh. As a result, arsenic concentrations have been strictly determined to be less than 10 μg/L and 1.5 μg/L in freshwater and seawater by the WHO, respectively [30]. However, in Bangladesh arsenic has an extremely high concentration level in the hydrosphere caused the regular concentration has to be limited under concentration in 50 μg/L [31-32]. In the beginning 1970s, there are around 10 million hand-pumped wells were installed to avoid pathogens through waterborne prevalent in Bangladesh, however, arsenic contamination in those wells was ignored until about 35-77 million people have been chronically exposed to increased concentrations of arsenic through drinking water in 1990s [33]. Moreover, many studies have been reported on persistent arsenic exposure to drinking water gradually increased mortality rates from chronic diseases in Bangladesh [34-35]. Thus, arsenic removal technologies are requested for preventing food safety and human health from toxicity.

1.2 Applications of absorbent for water treatments

The removal of conventional and urgent contaminants in drinking water and wastewater treatment plants depends on the physicochemical properties of the contaminants and the treatment process [36]. There are many existing water treatment technologies, such as oxidation method, membrane technology, ion exchange, electrochemical method, and adsorption method [37-40]. Among these technologies, the adsorbent is the most widely employed method for drinking water treatment technologies owing to absorbent materials are abundant existing in nature, easy to be extracted, low cost, easy to degradability, and friendly to nature, thus it is reported to remove kinds of organic substances, heavy metal ions, and complex pollutants in water treatment progress [41-45].

1.2.1 Absorbents for radioactive substances

Absorbents for removal of multiple radioactive substances have been studied, such as M.I.A.Abdel Maksoud et. al. studied the removal of ^{134}Cs and $^{152+154}Eu$ using modified bismuth tungstate from the aqueous solutions [46-47]. They believed that the bismuth tungstate has high electrical conductivity, excellent adsorption layer, extraordinary chemical stability, which have effective adsorption of contaminants from aquatic environments [48-49]. Zeolitic imidazolate framework also can be used as a basic organic absorbent for the absorption of radioactive substances and heavy metals from the water environment [50]. Absorbents for water treatment are the generality of

high polymer material, high surface area (porous or spherical structure), and functional group with hydroxy and carboxyl [51-53]. Seaweed had already been reported as an index plant for estimating radionuclides concentration in seawater. T. Yutaka et. al had investigated that the growth place of *sargassum horneri* is an indicator for evaluating ^{90}Sr concentration in seawater, the luxuriant *sargassum horneri* discovered represents a high concentration of ^{90}Sr existing in the water resources [54]. J. Burger et. al also mentioned that assessment of the concentration of radionuclides could rely on the habitat of marine organisms like *seaweed*, or s*argassum horneri* [55]. In a word, radionuclides could supply the nutrients for the marine organisms, thus, some studies have shown that ^{90}Sr and ^{79}Se can be effectively removed from seawater using absorbent of alginate or modified alginate [56-58].

In this research, we would like to apply alginate, which was extracted from seaweed as one kind of basic absorbent for removing radioactive substances from seawater. The reason for using seaweed is because the chemical structure of *seaweed* or *sargassum horneri* contains alginate, which is consisting of a copolymer of 1, 4-linked α-D-mannuronic (M) and β-L-guluronic (G) [59-60]. The chemical structure of

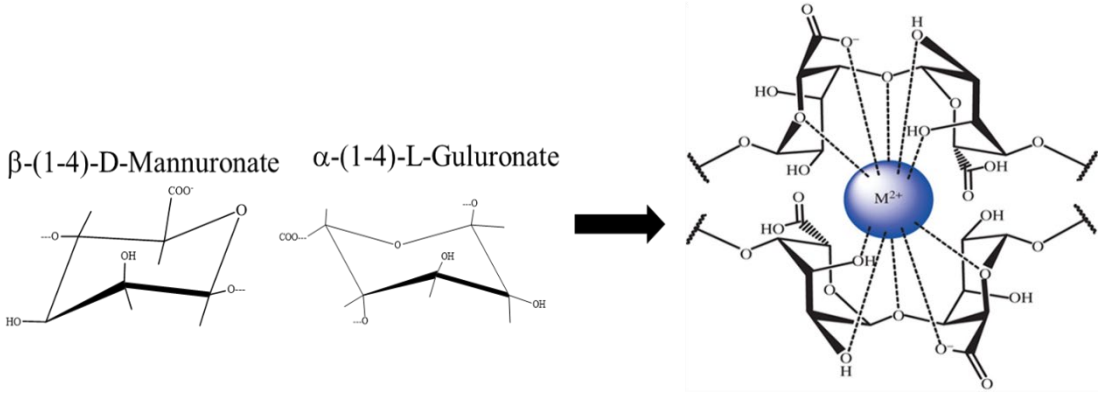

Figure 1.1 The “egg-box” structure of alginate with divalent cations.

alginate contains functional groups of hydroxyl and carboxyl groups, which can capture the cations and divalent cations in water bodies [61-62]. As the alginate and cations bind continuously, the chemical structure will change from straight-chain to spherical as in Figure 1.1 shown. While alginate captured divalent cations, it formed like an egg box model, cations are surrounded by alginate [59]. Therefore, alginate had been studied as useful absorbents to absorb cations such as Pb^{2+}, Cu^{2+}, Ni^{2+}, Cd^{2+}, and Cr^{3+} in the liquid phase [59]. Additionally, some researchers reported that the species, age, location, and environment of growing up of alginate would change its sequence caused the species of cations capture would be changed [60]. Song. et. al. found that Ca-alginate beads have a special ability to absorb Sr^{2+}, Li^{+}, and various metals in an aqueous solution because the hardness of alginate would be much stronger while other absorbates are cached [61]. H. Hye Jin referred to MnO_2 modified alginate beads could increasing the capacity of alginate absorption owing to the formation of alginate changed into a cycloid [62]. Based on those previous researches, alginate has been shown as a great potential absorbent for the removal of radioactive substances.

1.2.2 Absorbents for heavy metals and arsenic

Besides alginate, α-amylose also shows potential for absorbing divalent metal ions from water environments. α-amylose is one kind of sugar chain and normally exists inside the stem of rice species, such as reed, miscanthus, lemongrass, and so on [63-65]. Moreover, α-amylose is easily extracted from starch and cellulose. As we all know, starch is an abundant, low-cost, biodegradable, and renewable nature polymer [66-67]. The backbone of α-amylose has a substantial number of reactive hydroxyl groups that

easy can be attracted with heavy metal ions, the structure is shown in Figure 1.2. There are some researchers have reported that sugar chain polymer presence can absorb heavy metals ions from the aqueous environment. Chitosan is also one kind of sugar chain species, the structure of chitosan shows the number of hydroxyl groups, which has the same property as α-amylose [68-69].

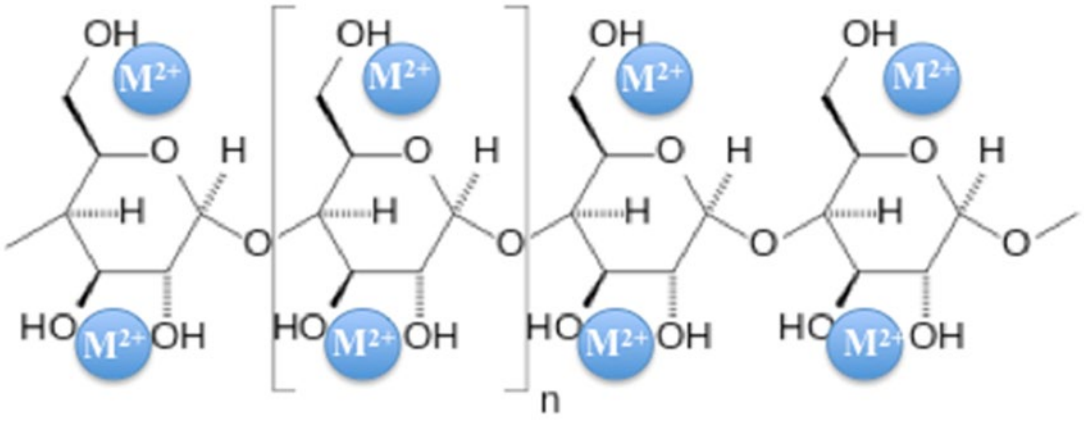

Figure 1.2 the structure of α-amylose bonding with heavy metals cations

Y. Ren refers to magnetic EDTA-modified chitosan with SiO_2 and Fe_3O_4, which increased chitosan sorption efficiency for removing heavy metals from water [70]. However, they found that since chitosan had been synthesized with SiO_2 and Fe_2O_4, the pH has been changed to a very low value resulting in low adsorption efficiency [71]. Moreover, Pb^{2+} in water bodies could be absorbed using glucose solution on thiol-functionalized cellulosic biomass due to glucose also has the same character as □-amylose [72]. This method showed that using wood sawdust and buckwheat hull could absorb Pb^{2+} without loss of glucose in solutions because sawdust and buckwheat hull contains hydroxyl groups as well [73]. Although many researchers found a-amylose,

chitosan, and glucose have potential adsorption of divalent metal ions, those absorbents have limitations, such as pH controlling conditions; surface capacity limitation, and so on [74-76]. A. Nabil discovered that through chelation modified cellulose could increase heavy metal ions adsorption with less pH control compare with no modification [77]. Y. Li et. al. found that dithiocarbamate-modified starch has a high performance for heavy metal adsorption because the carboxyl group was bonded with the hydroxyl group [78]. Although, the modified absorbent could ignore pH conditions has the best affinity with cations in a water environment, □-amylose contained absorbents still are requested to increase their sorption capacity based on the previous studies.

In addition, α-amylose and other sugar chain have been studied for arsenic adsorption in water resources as well [79]. Arsenic commonly has As (III), As (V) forms, and other complex forms in water bodies, iron salts, aluminum salts, and other cations salts can form hydroxides that combine with arsenic ions in aqueous solutions [80-81]. Therefore, some studies found that As (III) is much easier to remove compared to As (V) form [82-83]. Ferromanganese oxide as an absorbent for removing arsenic has been studied owing to it has porous structure and large surface area [84]. Manganese has a function for converting As (III) to As (V) [85]. Although the efficiency of using ferromanganese showed a great performance, the high-cost and complex synthesis method caused limitations [86]. S. I. Siddiqui et. al. reported that they were using starch functionalize maghemite as an adsorbent for arsenic removal from water resources, they found that it exhibited a good adsorption activity for As (III) [89]. In water bodies,

arsenic is not only the one ion matter existing but also other organic and inorganic substances here. H. Chen et. al. have studied the removal of arsenic and cadmium from water using Cs^{2+} modified starch-stabilized ferromanganese, it has been found that two substances could be removed simultaneously, but a certain pH value is requested [90]. Therefore, there is no study on removing arsenic and other heavy metals without synthesized starch and pH control.

1.3 Application of the electrochemical method in absorption

As the previous paragraph mentioned, carbon materials are used as absorbents for water treatment due to their high surface and functional group existence as well. For example, activated carbon has been reported to be an excellent absorbent for heavy metals removal because of its porous structure, high specific surface area, and functional groups existing [91]. Besides activated carbon, biochar, carbon fiber, and carbon nanotubes are been studied in quantity as absorbents for water treatment [92-94]. These carbon materials have common properties as absorbent, such as abundant existing in nature, low cost, easily degradable, and functional groups of $COOH^-$ existing [95-97]. However, many studies reported that bulk carbon materials utilization has a few disadvantages, like absorption limitation, secondary treatment requested, and pH controlling [98-99]. Thus, A. Nasrullah et. al mentioned that alginate impregnating with activated carbon could enlarge the sorption capacity compare to bulk carbon materials owing to absorbents could work simultaneously [100].

On the other side, many researchers have reported that some carbon materials could be used for adsorption with electrochemical methods because of good electroconductivity [101]. Graphene is one of the well-known carbon materials, which has high electroconductivity and multi-layer sheet structures [102]. The mechanism of high electroconductivity of graphene is carbon atoms have six electrons totally, two atoms in the inner shell and four atoms in the outer shell [103]. And four outer shell electrons in a carbon atom could be used as chemical bonding [103]. However, in graphene, three other carbon atoms on the second-dimensional plane connect with each atom, one electron will be left for electronic conduction in the third dimension [104]. Those highly mobile electrons are located above and below the graphene sheet. The property of electrons of graphene depends on electron bonding and anti-bonding [105]. G. Gollavelli et. Al. mentioned that magnetic graphene could remove organic and inorganic matters such as E-coil and heavy metal ions simultaneously, it has shown a great performance of adsorption efficiency in heavy metal removing, but still consumed time to remove all toxic matters [106]. Therefore, it is necessary to find a good carbon material, which has adsorption and high electroconductivity property.

1.4 Adsorption isotherms study

Pollution absorption plays an important role and is the most useful method in aqueous solutions, as the development of absorption reduces many steps in wastewater treatment [107]. The design of a highly efficient absorption system influences the result of water treatment progresses. Moreover, the effectiveness of low-cost absorption

materials can be judged from various aspects such as absorption volume, rate, etc [108]. So many studies have shown to understand the absorption principle and process, most often using absorption isotherms to evaluate the performance of absorption materials in the absorption processes [109-110]. Figure 1.3 shows the different types of isotherms that have been reported in various applied sciences and engineering fields, each type of isotherm is expected to depend on the nature of the adsorbent-adsorbent system, with Type I (Langmuir isotherm) being widely accepted for unconventional resources, such as gas absorption, organic and inorganic substances absorption from solid and liquid phase [111-113].

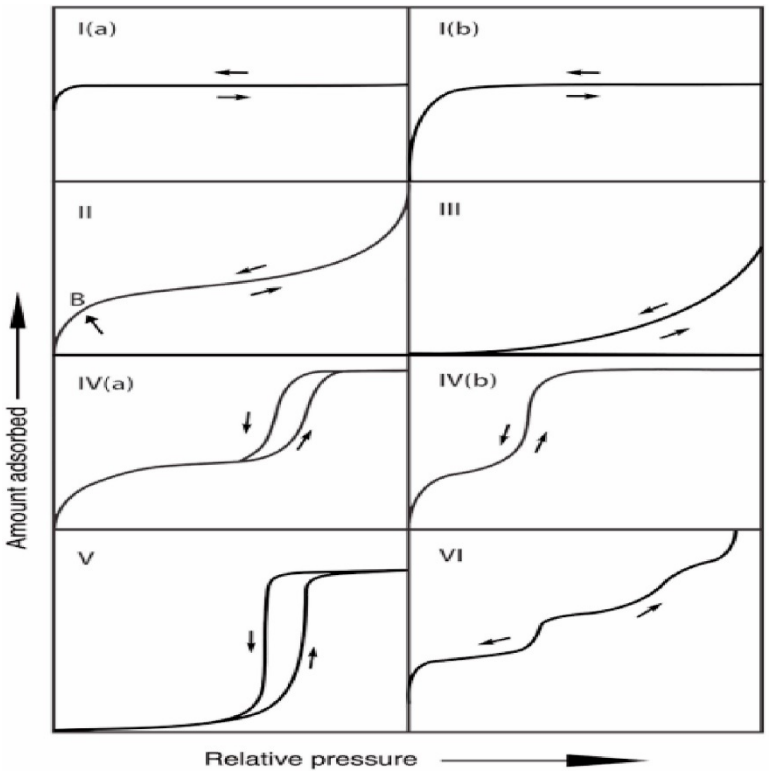

Figure 1.3 Classification of absorption isotherms (IUPAC technical report 2015)

The adsorption isotherm is an important parameter in the study of chemisorption processes to understand its factors affecting the rate and efficiency of absorbent. It is necessary to constantly monitor the rate of the influencing chemical reactions

repeatedly in experiments to find the absorption equilibrium reached in a given time [111]. The rate of absorption depends on the concentration of absorbent and absorbate involved in the chemical reaction [112].

In 1916, Irving Langmuir published his classical equation, and because it was initially used only to study the adsorption behavior of gases at the solid interface when gas molecules hit the surface, they are held near the surface by intermolecular attraction, and this bonding is similar to condensation. They are kept near the surface by intermolecular attraction, but for a short and limited time until they enter the bulk gas phase again, similar to evaporation (Figure 1.4). The Langmuir adsorption isotherm equation is defined as:

$$\theta = \frac{KP}{1+KP} \quad (1)$$

Where θ represents the coverage of the surface site of absorbent for gas adsorption, P

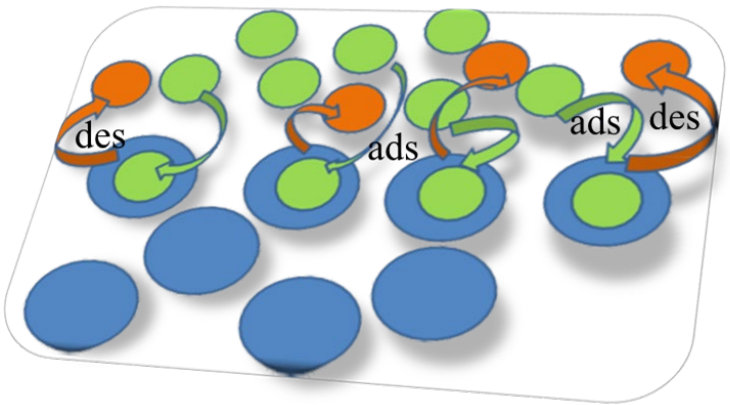

Figure 1.4 The kinetic model of Langmuir of adsorption acknowledges occurring between gas at equilibrium with a surface: adsorption (ads), and desorption (des).

is the pressure of the gas phase at the equilibrium value, K is the Langmuir constant value at the equilibrium pressure. And the model shows the relationship between absorbent site (absorbed gas) and free gas pressure. However, the Langmuir model was developed based on the assumption of monolayer sites and that no interactions between adsorbed molecules occurred. Moreover, this model only considered the low-pressure concentration uptaken, this assumption may not be satisfied higher pressures encountered, thereby limiting the predictive power of the Langmuir model.

A major problem in the Langmuir model is the assumption that the surface of the adsorbate is homogeneous. In 1998, it was shown that the model is not valid for inhomogeneous [113]. Therefore, the calculation of the adsorption capacity of adsorbent materials with similar porous non-uniform surfaces is flawed.

The Langmuir model assumes the phenomenon of monolayer adsorption. Initially, as it was used in the gas adsorption model, it could be assumed that a gas molecule was adsorbed on a single adsorption site and no other molecule could be on top of it. But later on many studies have proved that adsorbed gases are not only monolayer adsorption either, and in 1938 the BET model was developed, which can be said to be an extension of the Langmuir model to specifically account for the adsorption phenomena attributed to the presence of multiple layers, meaning that the molecule being adsorbed as an adsorption point itself allows for an increase in adsorption capacity [114]. Similar to the Langmuir model, the BET model assumes a homogeneous surface and negligible lateral interactions between the adsorbed molecules [115-116]. The BET equation could be written as:

$$\frac{P}{V(P_0-P)} = \frac{1}{V_m K} + \frac{K-1}{V_m K} \times \frac{P}{P_0} \quad (2)$$

Where *Vm* is the maximum monolayer adsorption volume, *V* is the adsorption volume at equilibrium, *K* is a constant value for adsorption, P is the free pressure of the gas and P_0 is the saturated pressure of the gas. For porous adsorption materials, the BET-based model of the adsorption process was shown to be more consistent with the adsorption amount than the conventional Langmuir model [117].

The Langmuir model assumes a constant maximum gas volume for the same adsorption material under isothermal conditions [118]. However, in 1991, an inverse relationship between the total amount of gas adsorbed and the temperature was found. When performing adsorption experiments is, the effect of temperature cannot be ignored, especially when the experimental conditions from gas to other phases.

As a result, if the adsorbent material is porous and has an irregular shape or if external forces are used to change the original adsorption rate, there are data defects in using this model to calculate the adsorption amount. Therefore, a derivation based on this model is needed to establish a new calculation formula.

1.5 Objectives and outline of the thesis

1.5.1 The objective of the thesis

In this study, we firstly investigated radionuclide of Sr^{2+} and several kinds of common heavy metal contaminants, absorption to porous graphite and porous graphite impregnated with alginate, α-amylose based on electrostatic interaction, respectively. Second, we conducted arsenic absorption using starch added a graphite porous carbon

plate, and real water sampling in Bangladesh to carry out arsenic compounds removal experiments from local drinking and river water. The electrochemical method in this study has been widely used in the removal of the toxic contaminants from water resources due to anion and cation interaction between the surface of absorbents with Sr^{2+}, heavy metal ions and arsenic compounds, which is similar to electrostatic repulsion and electron attraction.

1.5.2 Outline of the thesis

The main body of this thesis is dived into six chapters.

Chapter 1 describes the general background of this study. Alginate and α-amylose function as absorbents are discussed in detail. Due to both bulk absorbents having a limitation of sorption capacity, porous carbon materials were added to enhance the surface area of the absorbent and there is another benefit for carbon material based on the good electro-conductivity. Furthermore, the benefits of using the application of the electrochemical method were described as well. And the objectives and outline of this thesis were described.

Chapter 2 explains the experimental mechanism of the utilization of the instrument during studies. Firstly, the procedures of electrochemical measurement for Sr^{2+}, heavy metal, and arsenic compounds absorption were explained. Secondly, the benefit of the Scanning Electron Microscope (SEM), Raman spectroscopy, X-ray Diffraction (XRD), and 3D Laser Spectroscopy applied for characterization of carbon material was described individually. Finally, Atomic Absorption Spectroscopy (AAS) and

Inductively Coupled Plasma (ICP) for water analysis were discussed.

Chapter 3 describes the evaluation of the strontium (Sr^{2+}) sorption using an alginate/TiO_2 doped porous carbon electrode. The characterization of the carbon materials by SEM and Raman spectroscopy was examined for optimized carbon species determination. Alginate optimizes particle size was measured using the gel-sol phase critical line. And the comparison of the sorption efficiency of bulk alginate and alginate/ TiO_2 doped porous carbon was evaluated to invest a potential absorbent for Sr^{2+} absorption from water.

Chapter 4 describes the characterization of the common four heavy metal ions absorption using α-amylose/TiO_2 doped porous carbon electrode. Also, the optimized concentration of α-amylose was discussed by the vaccum system. A new absorption isotherm was developed based on the Langmuir isotherm equation for evaluating the new absorbent absorption potential. Furthermore, a comparison of individually heavy metal absorption amount with mixed heavy metal was discussed. And the new method for composting the new absorbent was also discussed in the final.

Chapter 5 describes the characterization of the arsenic sorption using starch added TiO_2 doped porous carbon electrode. The real water and rice samples from Bangladesh were analyzed using the ICP and figured out the arsenic concentration in daily consume water. The arsenic removal experiments from standard and real water solutions were discussed as well. The optimized concentration of starch application was discussed based on comparison experiments. And the optimized potential charge was also discussed regarding the absorbed amount value of arsenic.

Chapter 6 describes the general conclusion of this thesis. And the future predictions of this study have also were been discussed.

1.6 References

[1] H. S. Park, C. Ji, T. H. *Build Environ.* 95 (2016) 113-114

[2] M. Pizzol, P. Christensen, J. Schmidt, M. Thomsen, *J. Cleaner Pro.* 19 (2011), 646-656

[3] J. Rovira, J. Domingo. *Environ. Res.* 168 (2019), 62-69.

[4] L. Flandroy, T. Poutahidis, et. al. *Sci. Total. Environ.* 627 (2018), 1018-1038.

[5] O. M. L.Alharbi, A. A. Basheer, et. al. *J. Mol. Liquids* 263 (2018), 442-453.

[6] L. Ritter, K. R. Solomon, et. al. *United Nations Environment Programme* 2007.

[7] P. Rao, S. kodavanti, et. al. *International Encyclopedia of Public Health* 2017, 359-366.

[8] S. M. Rodrigues, P. F. A. M. Romkens. *Soil Pollutant* 2018, 217-250.

[9] Q. Gao, J. Xu. et. al. *Coord. Chem. Rev.* 378 (2019), 17-31.

[10] S. Li, Y. Chen. et. al. *Chin. J. Chem.* 34 (2016), 175-185

[11] E.O.Alamu, A.Mooya, *Smart Technologies for Sustainable Smallholder Agriculture* 2017, 201-210.

[12] A. Ruckert, R. Labonte, *Soc. Sci. Med.* 187 (2017), 306-311.

[13] K. E. Smith, C. Bambra, et. al. Health Inequalities: Critical Perspectives. 2015, 164-176.

[14] A.P. Black, J. Brimblecombe. et. al. *BMC Public Health.* 12 (2012), 1099.

[15] C.M. Heflin, K. Siefert, D.R. Williams. *Soc. Sci. Med.*, 61 (2005), 1971-1982.

[16] M. Karanikolos, P. Heino, nt. *J. Health Serv.*, 46 (2016), 208-240.

[17] A. Kentikelenis, I. Papanicolas, *Eur. J. Public Health*, 22 (2011), 4-5.

[18]S.I. Kirkpatrick, L. McIntyre, M.L. Potestio,*Arch.Pediatr.Adolesc.Med.*, 164 (201 0), 754-762.

[19] R. Labonté, Can. J. Public Health Rev. Can. Santé Publique, 100 (2009), 173-175.

[20] M. Lawson The World Bank and Inequality: from Poverty to Power (2016).

[21] A. Ruckert, R. Labonte, *Crit. Public Health*, 22 (2012), 267-279.

[22]A. Ruckert, R. Labonté, R.H. Parker, *Handbook of Healthcare Policy and Governance*, Palgrave Macmillan UK, London (2015), 37-53.

[23] C.J. Ruhm, *Q. J. Econ.*, 115 (2000), 617-650.

[24] Sustainability Commission Report [WWW Document] (2015)

[25] F. Parvin, S. Y. Rikta, et. al. *Nanotechnology in Water and Wastewater Treatment* 2019 137-157.

[26] K. Pyrzynska, *Environ. Chem. Eng.* 7 (2019),102795.

[27] C.F. Carolin, P.S. Kumar, et. al. *J. Environ. Chem. Eng.*, 5 (2017), 2782-2799.

[28] F. Shakerian, K.H. Kim, et. al. *Trends Anal. Chem.*, 82 (2016), 55-69.

[29] K. Attar, D. Bouazza, et. al. *J. Environ. Chem. Eng.*, 6 (2018), 5351-5360.

[30] S. Sen Gupta, K.G. Bhattacharya, *Adv. Colloid Interf. Sci.*, 162 (2011), 39-58.

[31] R. Zafar, K.M. Zia, et. al. *Int. J. Biol. Macromol.*, 92 (2016), 1012-1024.

[32] G.Z. Kyzas, M. Kostoglou, *Materials*, 7 (2014), 333-364.

[33] K.R. Yadanaparthi, D. Graybill, R.von Wandruszka, *J.Hazard. Mater.*, 171 (2009),

1-15.

[34] L. Cutillas-Barreiro, R. Paradelo, et. al. *Ecotoxicol. Environ. Saf.*, 131 (2016), 118-126.

[35] N. Kim, M. Park, D. Park, *Bioresour. Technol. Rep.*, 175 (2015), 629-632.

[36] L. Cutillas-Barreiro, L. Ansias-Manso, et. al. *J. Environ. Manag.*, 144 (2014), 258-264.

[37] D. Mohan, H. Kumar, et. al. *Chem. Eng. J.*, 236 (2014), 513-528.

[38] A.M.A. Pintor, C.I.A. Ferreira, *Water Res.*, 46 (2012), 3152-3166。

[39] M. López-Mesas, E.R. Navarrete, *Chem. Eng. J.*, 174 (2011), 9-17.

[40] V.K. Gupta, A. Nayak, *Chem. Eng. J.*, 180 (2012), 81-90.

[41] A. Almasi, M. Omidi, *Toxicol. Environ. Chem.*, 94 (2012), 660-671.

[42] P.S. Kumar, S. Ramalingam, *Clean – Soil, Air, Water*, 40 (2012), 188-197.

[43] W.E. Igwegbe, B.C. Okoro, *Int. J. Environ. Ecol. Eng.*, 9 (2015), 1410-1414.

[44] N.K. Akunwa, M.N. Muhammad, *J. Environ. Manag.*, 146 (2014), 517-523.

[45] Q. Li, L. Chai, W. Qin, *Chem. Eng. J.*, 197 (2012), 173-180.

[46] C. Suresh, D.H.K. Reddy, *Sci. World J.*, 154809 (2014).

[47] M. Jain, V.K. Garg, *Int. J. Environ. Sci. Technol.*, 13 (2016), 493-500.

[48] L. Cutillas-Barreiro, R. Paradelo, et. al. *Ecotoxicol. Environ. Saf.*, 131 (2016), 118-126.

[49] A. Aghababaei, M.C. Ncibi, M. Sillapää, *Bioresour. Technol. Rep.*, 239 (2017), 28-36.

[50] A. Abdolali, H.H. Ngo, et. al. *Sci. Total Environ.*, 542 (2016), 603-611.

[51] A. Dutta, Y. Diao, et. al. *J. Environ. Eng.*, 142 (2016), 1-6.

[52] B.O. Jones, O.O. John, *J. Environ. Manag.*, 177 (2016), 365-372.

[53] Y. Liu, X. Sun, B.U. Li, *Carbohydr. Polym.*, 81 (2010), 335-339.

[54] A. Saraeian, A. Hadi, *J. Environ. Chem. Eng.*, 6 (2018), 3322-3331.

[55] X.Y. Guo, S. Liang, *Adv. Mater. Res.*, 236-238 (2011), 237-240.

[56] P. Regmi, J.L. Garcia Moscoso, J. *Environ. Manag.*, 109 (2012), 61-69.

[57] M. Ahmad, S. Ahmed, *Int. J. Pharmacog.*, 2 (2015), 280-289.

[58] G.Z. Kyzas, D.N. Bikiaris, *Mar. Drugs*, 13 (2015), 312-337.

[59] L. Zhang, Y. Zeng, Z. Cheng, *J. Mol. Liq.*, 214 (2016), 175-191.

[60] M. Arvanad, M.A. Pakseresht, *J. Chem. Technol. Biotechnol.*, 8 (2013), 572-578.

[62] G. Yang, L. Tang, X. Lei, *Appl. Surf. Sci.*, 292 (2014), 710-716.

[63] Y. Ren, H. A. Abbood, et. al. *Chem. Engin. J.* 226 (2013) 300-311.

[64] Z. Wu, Z. Cheng, *Bior. Tech.* 104 (2012) 807-809.

[65] P. Pal, A. Pal, *Int. J. Biol. Macromol*., 14 (2017), 1548-1555.

[66] A. Shekhawat, S. Kahu, *Int. J. Biol. Macromol.*, 104 (2017), 1556-1568.

[67] A.K. Mishra, A.K. Sharma, *Inter. J. Biol. Macromol.*, 49 (2011), 504-512.

[68] A. Chen, G. Zeng, et. al. *Chem. Eng. J.*, 191 (2012), 85-94.

[69] N. A. Fakhre, B. M. Ibrahim, *J. Hazar. Mater*.. 343 (2018) 324-331.

[70] X. Li, H. Zhou, W. Wu, *J. Colloid Interface Sci.*, 448 (2015), 389-397.

[71] R. Whitton, F. Ometto, et. al. *Environ. Technol. Rev.*, 4 (2015), 133-148.

[72] R. C. Ewing, W. J. Weber, *Pro. Nucl. Energy,* 29 (1995) 63-127.

[73] A. Ahmadpour, M. Zabihi, et. al. *J. Hazard Mater*., 182 (2010), pp. 552-556.

[74] R. Akkaya. *Desalination*, 321 (2013), 3-8.

[75] R.D. Ambashta, M.E. Sillanpää. *J. Environ. Radioact.*, 105 (2012), 76-84.

[76] J.A. Arnal, J.C. Esteban, *Desalination*, 129 (2000), 101-105.

[77] D. Banerjee, A. Rao Manjula, *Radiochim.* Acta (2017), 341-346.

[78] Y. Tateda, J. Misonou, Denryoku Chuo Kenkyusho Hokoku. 20 (1998), 1-4.

[79] J. Burger, M. Gochfeld, et. al. Health Physics. 92 (2007) 265-279.

[80] A. Yipmantin, H.J. Maldonado, et. al. *J. Hazard. Mater.*, 185 (2011), 922-929.

[81] R. Whitton, F. Ometto, et. al. *Environ. Technol. Rev.*, 4 (2015), 133-148.

[82] W.M. Ibrahim, *Hazard. Mater.*, 192 (2011), 1827-1835.

[83] H. Chen, Z. Chen, et.al. *J. Hazard Mater.*, 347 (2018), 67-77.

[84] Y.-J. Gao, M.-L. Feng, J. Mater. Chem. A, 6 (2018), 3967-3976.

[85] L. Fuks, D. Wawszczak, *Radiochemistry*, 60 (4) (2018), 400-408.

[86] Gupta N.K., Sengupta A., *Radiochemistry*, 60 (4) (2018), 400-408.

[87] A Haug, O.Smidsrød, *Chem. Scand.* 24, (1970,)843 – 854.

[88] K.Y. Lee, D.J. Mooney, *Prog. Polym. Sci.*, 37 (2012), 106-126.

[89] J. He, J.P. Chen, *Bioresour. Technol.*, 60 (2014), 67-78.

[90] F.V. Hackbarth, F. Girardi, et. al.*Chem. Eng. J.*, 242 (2014), 294-305.

[91] F.V. Hackbarth, F. Girardi, et. al. *Chem. Eng. J.*, 269 (2015), 359-370.

[92] T. Vincent , C. Vincent, *J. Mater. Chem. A*, 2 (2014), 10007-10021.

[93] S.V. Avery, *J. Ind. Microbiol*., 14 (1995), 76-84.

[94] A.K. Vipin, B. Fugetsu, et. al. *Sci. Rep.*, 6 (2016), 37009.

[95] K.Y. Lee, D.J. Mooney, *Prog. Polym. Sci.*, 37 (2012), 106-126.

[96] J. Choi, *Polym. Korea*, 41 (2017), 1046-1051.

[97] Y. Mihara, M.T. Sikder, *J. Water Process Eng.*, 10 (2016), 9-19.

[98] S.C. Jang, S.M. Kang, et. al. *Sci. Rep.*, 6 (2016), 38384.

[99] J. Yu, J. Wang, Y. Jiang, *Nucl. Eng. Technol.*, 49 (2017), 534-540.

[100] X. Li, H. Zhou, et. al. *J. Colloid Interface Sci.*, 448 (2015), 389-397.

[101] M. Moyo, S.T. Lindiwe, et. al. *Res. Chem. Intermed.*, 42 (2016), 1349-1362.

[102] N. Mohamed Nor, L.C. Lau, et. al. *J. Environ. Chem. Eng.*, 1 (2013), 658-666.

[103] I.I. Gurten, M. Ozmak, et. al. *Biomass Bioenergy*, 37 (2012), 73-81.

[104] U.I. Gaya, E. Otene, et. al. *SpringerPlus,* 4 (2015), 458-476.

[105]D. Obregon-Valencia, M.del R Sun-Kou, *J. Environ. Chem. Eng.*, 2 (2014), 2280-2288.

[106] T. M. Morales, N. Ganfound, *Ener. Storage Mater.* 2018.

[107] E. Raymundo-Piñero, K. Kierzek, *Carbon*, 44 (2006), 2498-2507.

[108] C. Largeot, C. Portet, *J. Am. Chem. Soc.*, 130 (2008), 2730-2731.

[109] S. Kondrat, A.A. Kornyshev, *J. Phys. : Condens. Matter,* 23 (2011), 022201.

[110] Y. He, J. Huang, B.G. Sumpter, *J. Phys. Chem. Lett.*, 6 (2015), 22-30.

[111] M. Sillanpaa, M. Shestakova, *Electrochemical Water Treatment Methods*, 2017

[112] X.Duan, L. Chang, *Environ Protect Chem. Ind.*, 30 (2010), 356-359.

[113] Q. Ke, *Environ Sustain Dev*, 40 (2015), 218-219.

[114] E. Ayrnaci, B.E. Conway, *J Appl Electrochem*, 31 (2001), 257-266.

[115] R. Chen, X. Hu, *J Colloid Interface Sci.,* 290 (2005), 190-195.

[116] P. Rana, N. Mohan, *C. Rajagopal, Water Res.*, 38 (2004), 2811-2820

Chater 2

Experimental

Chapter 2

Experimental

2.1 Materials and chemicals

Carbon materials: TiO_2 doped porous carbon, porous carbon, expanded carbon, black carbon, carbon graphite, and carbon fiber were donated by Hitachi Chemical Co., Ltd for electrochemical method utilization. Sodium alginate, soluble starch, copper (II) chloride, lead (II) chloride, cadmium (II) chloride were purchased from Wako, Japan. Chromium (IV) chloride hexahydrate and arsenic (As_2O_3) standard solution were purchased from Kanto Chemicals, Japan. Potassium chloride and sodium chloride were purchased from Wako, Japan as electrolytes in electrochemical method application. Hydrochloric acid, sulfuric acid, nitric acid, potassium permanganate, potassium iodide, tin(II) chloride, iron(III) chloride were purchased from Wako, Japan for arsenic analytic experiments and starch extraction from reed. All chemicals used in this study are analytical grade.

2.2 Electrochemical measurements

This research was used electrochemical methods to enhance Sr^{2+} radioactive species, heavy metals, and arsenic compounds for chemisorption by using absorbents with graphite porous carbon plates. The electrochemical method is an essential method for the electrochemical driving force in this study. The electrochemical method is applying the different potentials and currents for two electrodes in the water with an

electrolyte solution. The Electron moves the positive charge towards to negative charge in the liquid phase based on the principle of electrostatic reaction when the potential or current force. Meanwhile, an oxidation-reduction reaction is occurring on the two electrodes surfaces. In general, electrochemical measurements present three electrodes: working electrode (WE), counter electrode (CE), and reference electrodes (RE) as in Figure 2.1. Based on the Gibbs energy of the electrode surface, the potential was controlled by the operational amplifier. Potential is directly translated to the applied voltage. However, the voltage is not determined but required zero as the standard. Therefore, the reference electrode provides zero as the standard. In the case of the Ag/AgCl (sat'd KCl) electrode, the standard potential is -0.226 V vs. the hydrogen standard electrode [1]. The current is recorded with the potential. The current is caused by electron transfer. Here, two-electron transfer processes occur at the interface between electrode and solution. The first electron transfer process is the *Faradaic reaction* [2]. If the material is reduced or oxidized, the electron moves from electrode or solution to solution or electrode, respectively. In this case, the amount of reduced/oxidized material can be estimated from the charge density calculated from the observed current density. Another electron transfer is namely *non-Faradiac reaction* [2]. Electron is stored into the electro-double layer formed at the solution side of the interface [3]. It is illustrated to capacitor according to Gauy-Chapman model. However, this study does not use either *Faradiac reaction* or *non-Faradaic reaction*. The control of the surface charge is used for the improvement of absorption capacity.

The electrochemical measurements in this study were conducted with three-electrode cells. Absorbents with TiO_2 doped graphite porous carbon plate as WE, TiO_2 doped porous carbon as CE, and Ag/AgCl (saturated KCl) as RE, respectively. To control the potential an Ivium potentiostat (Ivium Technologies, Poland) for Sr^{2+} absorption and an Electrochemical Instrument (EI, HOKUTO DENKO, HZ-7000) was applied for heavy metal and arsenic removal treatment. EI has much higher potential and current than Ivoim potentiostat, the initial concentration of absorbate dependent on the instrument application. The heavy metal and arsenic experiments were conducted from a high concentration. In this study, constant potential experiments mainly were conducted during the absorption process.

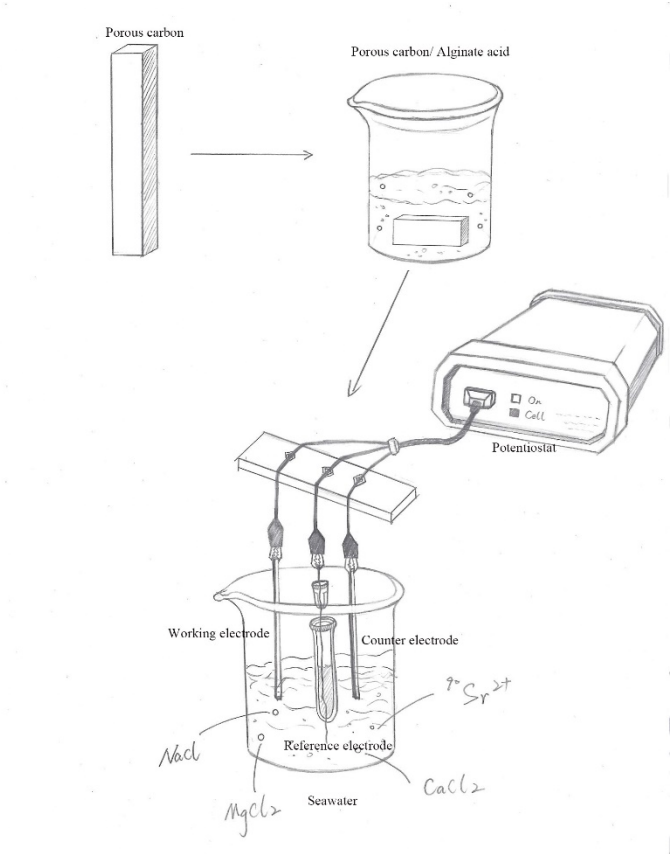

Figure 2.1 Typical three cells electrochemical measurement with the potentiostat.

2.3 Scanning electron microscope (SEM)

A Scanning electron microscope (SEM) is a machine for providing images of a sample by scanning the surface with a focused beam of electrons. The high-energy electron beam interacts with the sample materials to generate secondary electrons, back-reflected electrons, and X-ray signals. The signal emitted from any point on the surface of the sample corresponds to the corresponding bright spot on the fluorescent screen of the picture tube. Figure 2.2 shows a typically schematic SEM.

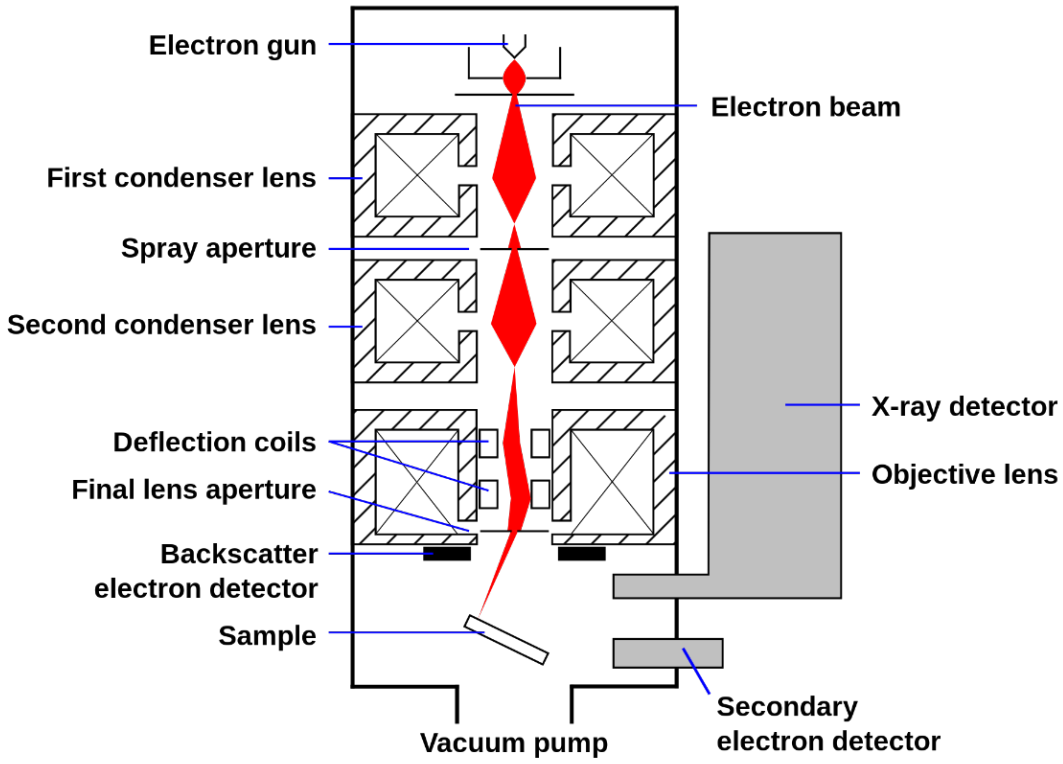

Figure 2.2 A typical SEM constitution scheme

[Ref.https://en.wikipedia.org/wiki/Scanning_electron_microscope]

In this study, to identify the structure of all carbon materials, the sample was cut into small pieces to observe section parts of samples. SEM images have been taken from Hitachi S4800 (Figure 2.3). For some carbon materials, because of its property

like carbon felt, the observation period is too long causing the carbon elements to absorb energy to increase the exposure intensity, resulting in the porous size cannot being judged correctly from the picture.

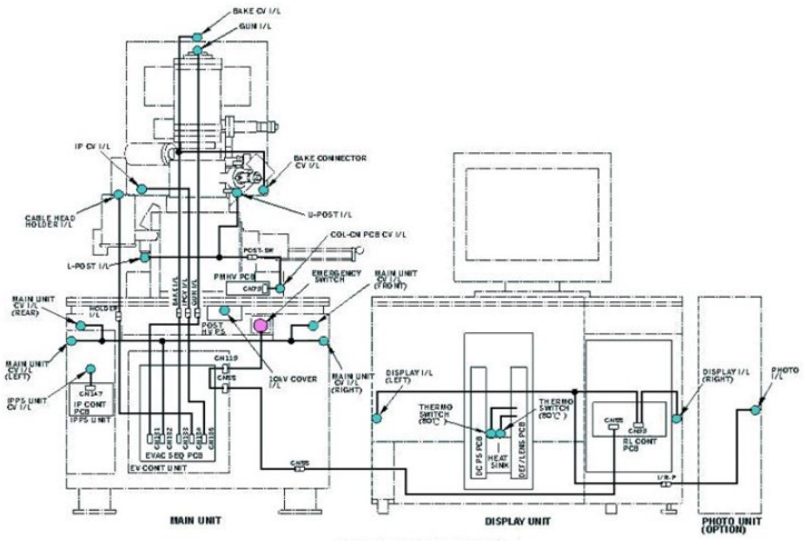

Figure 2.3 The composition of Hitachi SEM S4800 [6]

2.4 Ranman spectroscopy

Raman spectroscopy is a spectroscopic technique used to study the vibration modes, rotation modes, and other low-frequency modes in a system. Raman spectroscopy is a type of vibrational spectroscopy, which focuses on the chemical analysis of sample material composition by using light to create (excite) molecular vibrations that present a spectrum [7]. Raman is generally readily observed wavelength changes when using a monochromatic light source. After the interaction of monochromatic light with the material, it is possible to change a very small part of the wavelength, this change is called: the Raman effect, and finally, lights are collected and can be used to obtain the information of samples. Figure 2.3 shows the Ranman effect ranges, which are visible light, infrared light, and ultraviolet light. It occurs when light

strikes the molecule and interacts with electron clouds and molecular bonds in the molecule.

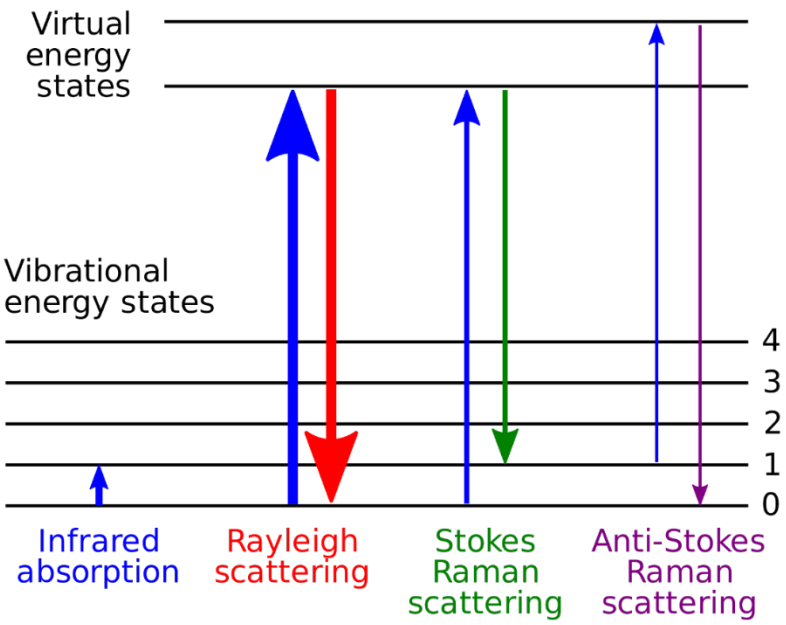

Figure 2.4 Energy level of Raman spectra range [7]

Raman spectroscopy has been described as an important tool for identifying materials for monitoring in various processes such as mixing homogeneity, granulation and drying processes, tablet evaluation, and coating monitoring. The vertical axis of Raman data usually has arbitrary and no units. This is because the exact value is simply a measure of the number of scattered photons captured by the detector during a specific time interval. The number of scattered photons captured by the detector at any given frequency in the spectrum over a specific time interval. If a sample is scanned *n* times, then the peak height will be *n* times higher. Similarly, if the incident laser power impinging on the sample is different, the intensity of the Raman spectrum will vary accordingly. Therefore, the peak height in Raman spectra is not a simple function of sample thickness, concentration, and Raman scattering properties, but also depends on

the laser power, laser wavelength, scanning time, sample orientation, etc [8]. In this study, carbon materials have been detected by JASCO RMP 500 Raman spectroscopy (Figure 2.5). Through the Ranman scattering strong well-defined bands of carbon materials, the structure of carbon could be identified.

Figure 2.5 The image of JASCO RMP 500 Ranman spectroscopy [8].

2.5 Atomic absorption spectroscope (AAS)

Atomic absorption spectrometry (AAS) detects elements in a liquid or solid sample by illuminating with excitation light of a specific wavelength from a light source. The principle of AAS is based on the fact that each atom absorbs excitation light of a specific wavelength. AAS is a method for quantitative of chemical elements based on the absorption of light by atomic vapors state. AAS can detect more than 70 different elements in the solution. The principle of AAS is that each atom absorbs light of a specific wavelength [9]. Excitation then causes the electrons of each atom to move up

one energy level as the atom absorbs specific energy in Figure 2.6 shown.

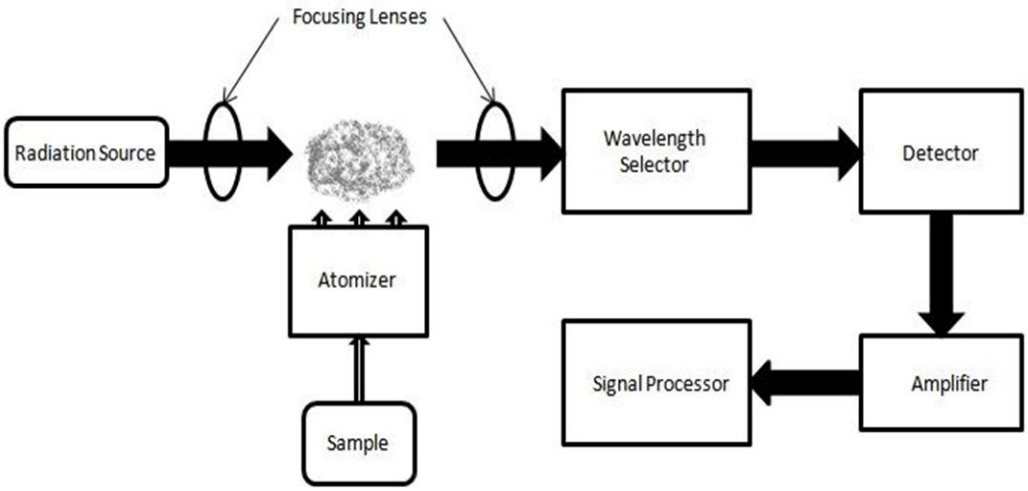

Figure 2.6 The principle of Atomic absorption spectroscope measurement. [9]

When the electrons return to their original energy state, the energy is emitted as light. This light has a wavelength that is unique to each element. Based on the wavelength of the light and its intensity, a specific element can be detected and its concentration can be measured [10-11]. AAS can be used in an infinite variety of applications and is still widely used for less complex trace element analysis. Flame Atomic Absorption Spectrometry (FAAS) has gained wide acceptance in many industries and continues to

Figure 2.7 The image of Hitachi Z- 2000 flame AAS.

be used due to its uniqueness and specific advantages. In this study, the concentration of strontium, copper, iron, lead, cadmium, and chromium have been determined by FAAS (Hitachi Z- 2000 Figure 2.7), respectively.

2.6 Inductively Coupled Plasma (ICP)

Inductively Coupled Plasma (ICP) is one of the elemental analyzers, which has a similar property to AAS. ICP is a type of ionization source that completely breaks down a sample into its constituent elements and converts those elements into ions. Commonly used is argon gas, it can reach to high temperature of 6,000°C to 10,000°C [12]. When a sample is introduced into the plasma, the elements in the sample are ionized. When a sample is introduced into the plasma, the elements in the sample are ionized, and these ions are sent to a mass spectrometer, where they are separated and detected according to their mass number (isotope), enabling qualitative and quantitative analysis of the elements. ICP has several advantages compared to FAAS, extremely high sensitivity, and ppt-level separation of elements without the influence of background spectra, such as arsenic compounds detection. The spectral range is relatively simple and qualitative analysis is easy. Furthermore, simultaneous multi-element analysis is possible compared to FAAS and rapid analysis can be performed. Isotope measurement is possible, and high-precision analysis is possible even at low concentrations by isotope dilution analysis [13]. Two points can be raised as problems as well: it is difficult to perform high-sensitivity and high-accuracy analysis for elements affected by overlapping background spectra; interference of coexisting elements is quite large, and

in general, desensitizing effects occur when the concentration of coexisting elements is several tens of ppm or more. In addition, matrix interferences are also large, and in cases where a large amount of salt is contained, the salt concentration is high. If it contains a large amount of salt, dilution is required until the salt concentration is about 0.1% [14].

In this study, due to the real samples being contaminated by several toxic heavy metals and organic compounds, moreover, to keep the accurate concentration from real water sample, the interrupt chemicals did not be added before detecting, thus, using the ICP analyzer instead of FAAS.

2.7 X-ray Diffraction (XRD)

X-ray diffraction (XRD) is widely used in research as a means of determining the state and physical properties of matters, most notably because it is based on the structure of a particular material at the molecular or atomic level, which is the smallest unit of physical properties [12]. The wavelength of the X-rays used in XRD is about 0.5 to 3.0 Å, and the diffraction is caused by the interference of X-rays scattered by electrons at the same distance. There are many characteristic methods of XRD depending on the condition of the sample and the purpose of the measurement, and there are a wide variety of ways to use them. Broadly speaking, these include powder XRD, single-crystal XRD, residual stress analysis, thin-film analysis, and small-angle X-ray scattering. The information obtained from powder XRD includes the identification and quantification of constituents, crystallite size, and crystallinity.

When X-rays with a wavelength of 0.5 Å to 3 Å, which is about the same as the distance between atoms, are incident on a material in which atoms are regularly arranged, the X-rays are scattered by electrons belonging to each atom [13]. The scattered X-rays interfere with each other and strengthen each other in a specific direction. The X-ray diffraction pattern obtained by powder XRD method the horizontal axis is the diffraction angle (2θ) and the vertical axis is the diffraction intensity (CPS). The diffraction angle 2θ depends on the lattice spacing d of the material, while the diffraction intensity depends on the arrangement of atoms and molecules and their species. The width of the peak is determined by the crystallinity, which depends on the size of the crystal grains and crystal distortion [14]. Qualitative analysis, which is a typical analysis method of powder XRD, identifies the crystalline phase by comparing the measured diffraction patterns with those of known materials, such as the XRD patterns of the unknown and known substances are compared to see if the positions and intensity ratios of each peak match, and if they do, these two substances are considered to be the same.

In this study, XRD was used to detect the graphite porous carbon material to understand the peak of XRD patterns and figure out the matters from the reference.

2.8 References

[1] A. Mahmood, W. Guo, H. Tabassum, R. Zou, Adv. *Energy Mater.*, 6 (2016), 1600423.

[2] A. Sankaran, C. Staszel, et. al. *Electrochem. Acta*, 268 (2018) 173-186.

[3]A. Castellanos, A.T. Perez, Handbook of Experimental Fluid Mechanics, *Springer*,

Heidelberg (2007), 1317-1331.

[4] M. A. Kanaparthi, S.D. *Cevaer, J. Aero. Sci.*, 126 (2018) 217-230.

[5] https://en.wikipedia.org/wiki/Scanning_electron_microscope

[6] https://www.hitachi-hightech.com/global/.

[7] O. I. Olubiyi, F. K. Lu, *Image-Guided Neurosurgery*, 2015, 407-439.

[8] https://en.wikipedia.org/wiki/Raman_spectroscopy

[9] R. Zahnow, J. M. Verigh, Inter. J. *Drug Policy*, 55 (2018) 105-112.

[10] Association Official of Analytical Chemists (AOAC International), Guidelines for Standard Method Performance Requirements (Appendix F), *AOAC Official Methods of Analysis* (2012), 1-17.

[11] E.G. Barrera, D. Bazanella, et. al. *Microchemical Journal* 132 (2017), 365-370.

[12] D.J.E. Costa, A.M. Martínez, et. al. *Talanta*, 154 (2016), 134-140

[13]Thamaphat, K., Limsuwan, P., & Ngotawornchai, B. (2008). Phase characterization of TiO_2 powder by XRD and TEM. *Agriculture and Natural Resources*, 42(5), 357-361.

[14] Marler, B., Oberhagemann, U., Vortmann, S., & Gies, H. (1996). Influence of the sorbate type on the XRD peak intensities of loaded MCM-41. *Microporous Materials*, 6(5-6), 375-383.

Chapter 3

Selective Removal of Strontium (Sr^{2+}) from Seawater by Using Alginate doped TiO_2 Porous Carbon Electrode

Chapter 3: Selective Removal of Strontium (Sr^{2+}) from Seawater by Using Alginate doped TiO_2 Porous Carbon Electrode

3.1 Introduction

Radionuclides wastes (^{136}Cs, ^{133}I, ^{90}Sr, ^{129}I) are toxically emitted from nuclear power plants disaster and nuclear fission [1]. They are reported to be the major health concern. Sr^{2+} is one of the highly toxic radionuclides which can be absorbed readily by crops and accumulated in the human body through the food chain, and so may represent an environmental threat to the health of the local population [2,3]. Meanwhile, one of the most universal problems is afflicting people throughout the world with insufficient access to clean water. Together with, the Fukushima Daiichi Nuclear Power Plant (FDNPP) accident, which was happened on 11 March 2011, led to serious water contaminations with radionuclides around FDNPP and neighboring prefectures [4]. Addressing these problems effective water remediation methods are of great importance to ecosystems and mankind.

Water remediation of radionuclides using traditional technologies such as membrane technology, ion exchange, adsorbents, and other technologies are expensive, inefficient, and non-selective adsorption [5,6]. Because of the high cost, cleansing of polluted water remains an intractable problem [7]. Adsorption with a variety of solid adsorbents is one of the most effective processes for a large volume of wastewater purification than other processes because of its high efficiency, fast and easy separation,

relatively cheap, and easily biodegradable [8,9]. Cs^{2+} adsorption using zeolite has been reported in many kinds of research [9-11]. I_2 removing from seawater by using active carbon also has been studied [12,13]. However, the appropriate selective removal of Sr^{2+} method from seawater is underdeveloped.

Sr^{2+} is considered as a hazardous radionuclide contaminant from the environmental standpoint, because of its relatively long half-life time (28.8 years), high volatility, high activity, and high solubility [14]. It would make competitivity with Ca^{2+} during the adsorption process because of the similarity of mobility rate, which is easy to be accumulated in bones and kidneys and eventually causes carcinogenesis as well [15,16]. Various methods of Sr^{2+} treatment from seawater have been studied such as precipitation, adsorption, and extraction [16-19]. However, those methods are inquired to secondary treatment and low-efficiency results [20,21]. Therefore, efficient and effective remediation methods are of great importance.

Here, we would like to pay attention to alginate as an adsorbent aiming to selective remove Sr^{2+} from seawater. Alginate is mainly extracted from *seaweed*, *seagrass*, and *sargassum*, and adsorption species are highly dependent on its ecological habitat, growing age, and gene sequence [22]. *Sargassum horneri* was investigated as an indicator of ^{90}Sr concentration in seawater [23]. J. Burger et al. also mentioned that *marine organisms* like *Laminariales*, or *Sargassum horneri* could be used for the assessment of the concentration of the radionuclides [24]. Alginate once captured radionuclides, an “egg-box” model could be formed a polymer chain with the function group of $COOH^-$ and OH^- [25]. Scheme 1 shows the “egg-box” model of alginate

absorbs mixed divalent ions from seawater. Alginate consists of a copolymer of 1, 4-linked α- D- mannuronic (M), and β- L- guluronic (G) [26]. The “egg-box” structure is dependent on the amount of G copolymer, the high G copolymer ratio much easier

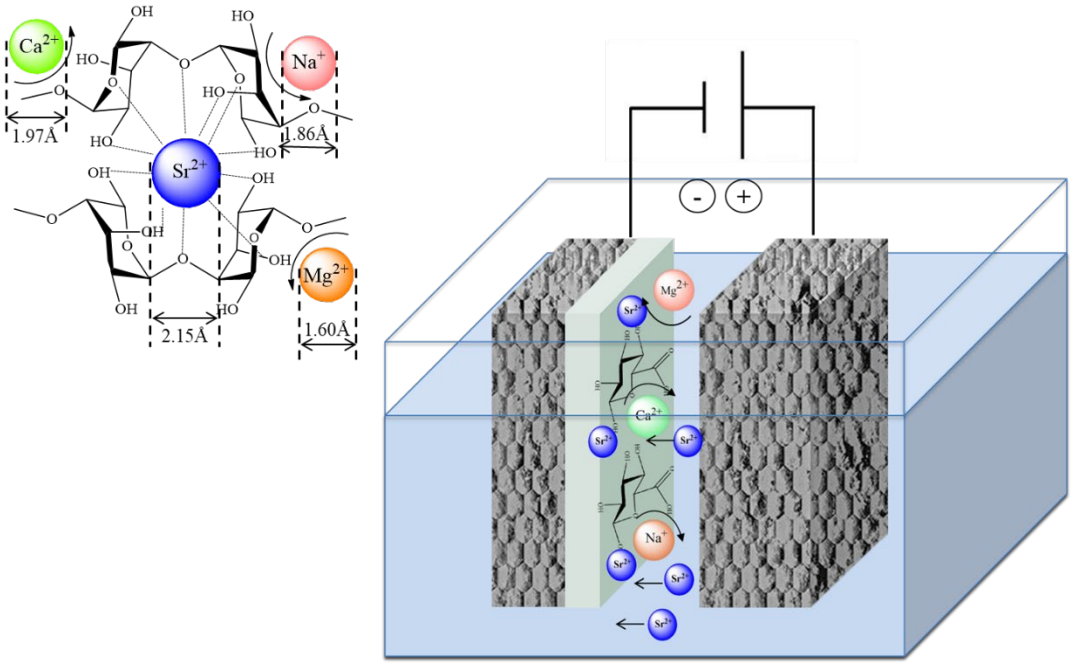

Scheme 1 Electrochemical system of Sr soption by doped alginate with TiO_2 doped porous carbon electrod, composite absorbent as working electrode; and TiO_2 doped porous carbon as counter electrode.

formed cross-linked reaction than high M copolymer ratio in alginate, meanwhile the “egg-box” exhibits high hardness when G copolymer majority existence in alginate [27,28]. The functional group of cross-linked points constructs a cavity of the bond, which has negative charges that contribute cations to move inside of polymer. However, there is no study of the cavity size of G copolymer, only the adsorption species, and the capacity. Competitivities of cations mixed the mobility of ions effect on alginate selective adsorption [29,30]. S. Dongsu et al. found that Ca-alginate beads have a

special ability to absorb strontium (Sr^{2+}), lithium (Li^{+}), and various heavy metals in aqueous solution [31]. H. J. Hong reported that MnO_2 modified alginate beads can increase the capacity of alginate absorption of strontium in seawater and other cations were released into the seawater with the alginate absorb strontium [32].

I also proposed the combination of an electrochemical method with Sr^{2+} using alginate doped porous carbon adsorbent to improve the negative charge of alginate takes effects on Sr^{2+} based on electrical interaction in this research. As scheme 1 showed in this research, absorbent alginate was doped into porous carbon through electrical interaction could selective absorb Sr^{2+} from seawater. The mobility of ion Sr^{2+} was straightforwardly captured by alginate from seawater and finally stock in the porous carbon based on the electrochemical method. Meanwhile, electrochemical methods have been studied for discharged water treatment and wastewater mediation as well, such as electrocatalytic reduction organic materials, electrochemical treatment for degradation of organic pollutants from wastewater [33,34]. There are many benefits for water treatment by using electrochemical methods, like no additional chemicals added, completely decomposing organic matters, and short operation time for water treatment [35-37].

Carbon materials combined with the electrochemical method have been investigated in many kinds of research. Graphite is one of the representative electrical conductive carbon materials, which is widely used to absorb a variety of heavy metals in past studies [38]. Moreover, many types of the research reported that the combination of graphite with functionalized materials showed remarkably high electroconductivity

and high efficiency of heavy metals adsorption [39,40]. Meanwhile, porous carbons such as biochar, carbon nanotubes, carbon fiber, and activated carbon are used as an absorbent medium in soil, air, and hydrosphere. Particularly, activated carbon has been reported that it is an excellent adsorbent for heavy metals adsorption owing to its porous structure, high specific surface area, and functional groups of $COOH^-$ [41]. Furthermore, there are some reports mentioned that alginate mix with activated carbon could increase the surface area of two adsorbents and adsorption capacity to heavy metals adsorption [42]. A. Nasrullah et. al. mentioned that due to limited absorption of activated carbon, it is impregnated with alginate would enlarge its adsorption capacity and high efficiency for heavy metals adsorption [43]. The electrophoresis method is wildly used in molecular biological and colloidal sciences in polymer gel medium [44]. When the particle in free solution migrated through the pores of a gel matrix, the short-range steric interaction will be occurred to separate individual molecules form a mixture under an electric field [45]. Therefore, we would like to propose a new adsorbent, which is alginate with graphite based on an electrochemical method to selectively absorb Sr^{2+} from seawater.

In this research, alginate doped into porous carbon using the electrochemical method applies to Sr^{2+} adsorption from seawater. Different alginate phases will be doped into the porous carbon, and a negative charge would be applied to porous carbon to improve the surrounded function group of alginate. Divalent ions in seawater would be attracted by alginate based on static interaction of electricity as in Scheme 1 shown, and the ions inside of porous carbon cannot secondary re-contaminate seawater. Overall,

we are aiming to propose a high-efficiency adsorbent to reduce secondary treatment and a selective removing Sr^{2+} from seawater.

3.2 Experimentals

3.2.1 Materials

All reagents used in this study were analytical grade. Standard solution of strontium chloride, Potassium chloride, and Sodium alginate (viscidity 300-400 cps) was purchased from Wako, Japan. Potassium chloride was added to avoid interferences and control the ionization of strontium when using an automatic absorption spectrophotometer. Porous carbon plates were donated by Hitachi Chemical Co., Ltd. Artificial seawater was obtained from Osaka Yakken Co., Ltd. (JIS12140).

3.3 Instruments

In this study,, the porous carbon plates characteristic were measured by scanning electrode microscope (SEM, Hitachi, S4800 series), X-ray diffraction (XRD, RINT2200V), Raman spectroscopy (JASCO, RMP 500), and a digital multimeter (ADVANTEST, R6450), respectively. And the Sr^{2+} sorption experiment was conducted by using an electrochemical instrument (Ivium compactstat, Ivium Technologies, Poland), which is connected to three electrodes. Alginate doped porous carbon plate, porous carbon plate, and Ag / AgCl electrode as working electrode (WE), counter electrode (CE), and reference electrode (RE), respectively (Scheme 1.). The Sr^{2+} concentration was measured by using an atomic absorption spectrophotometer (AAS,

Hitachi Z- 2000).

3.3.1 Characterization of porous carbon

SEM was used to observe the appropriate porous size of two types of porous carbon plates, which samples were controlled in magnification: 4000, working distance: 17.4 mm, acceleration voltage: 5KV, and Emission current: 10 μA condition. SEM image (Figure. 1) shows two different types of surface pore size of porous carbon plates, the cavity of the pore was measured in 5 μm.

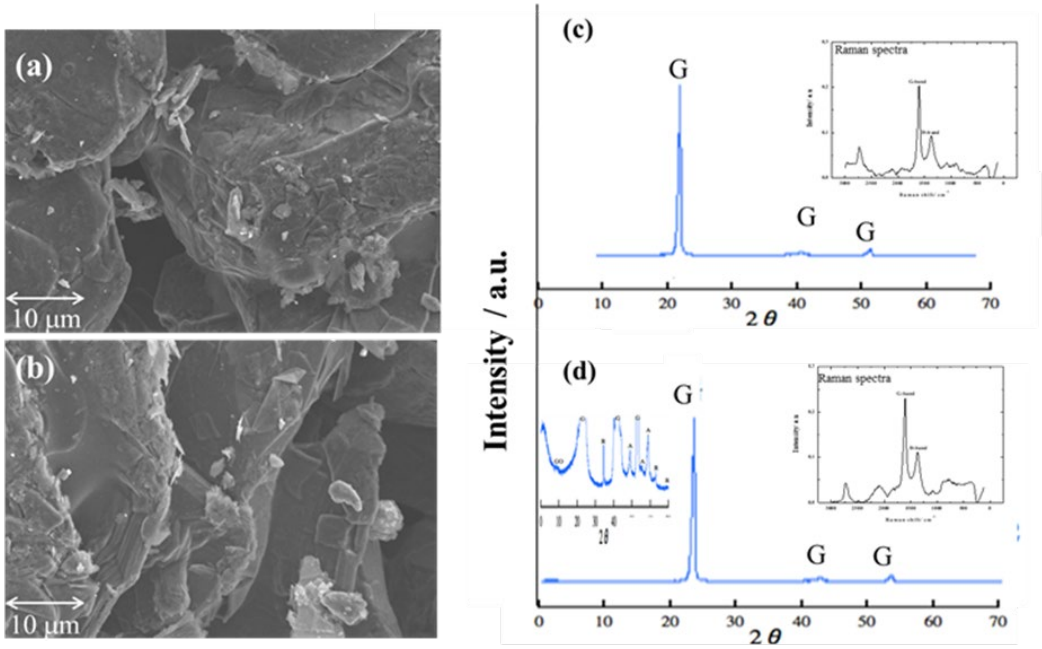

Figure 1. SEM imagines: (a) Porous carbon; (b) TiO_2 doped graphite porous carbon. (I: 10 mA V:5 kV Mag: 4000 WD: 17.4 mm)

X-ray diffraction and Raman spectra of: (c) Porous carbon; (d) TiO_2 doped graphite porous carbon.

According to the SEM images, two types of carbon plates exposed a similar pore size. It was noticed that carbon plates showed multi-layer formation. However, the formation of the material could not be identified from SEM images. Moreover, the structural

properties of carbon materials can be easily characterized via the atomic vibrations, which is depended on the bonds between the constituent atoms due to the physical properties of carbons that are correlated to the electronic configuration what is highly relied on the interatomic bond type [46]. XRD was used to detect the carbon crystal phase of two porous carbon plates using Cu-Ka radiation of 1.5405Å wavelength and a scanning speed of 2° min^{-1}. Raman spectroscopy (JASCO, RMP 500) was used to characterize the surface property of porous carbon electrodes as well. Raman spectroscopy is one of the widely used machines for detecting bond strengths via the lattice vibration in carbon materials [47]. Fig. 1 (c), (d) presents the XRD spectra and Raman spectra of two types porous carbon plates, through the results, two carbon plates were made of porous carbon and TiO_2 doped porous carbon, respectively. The observed XRD pattern was the XRD peak of graphite at $2\theta = 26.7°$, which is the same peak in literature [48]. Thus, two types of porous carbon are constituted by the graphite. In Raman spectra, the main feature of G-band and D-band appears at 1582 cm^{-1} and 1350 cm^{-1}, respectively [49]. The Raman peak around 1582 cm^{-1} is a typical Raman peak of bulk crystalline graphite, called the G-band [50]. This peak is the basic vibration mode of graphite crystals. The intensity is related to the size of the crystal. 1350 cm^{-1} peak value is derived from the vibration of the crystalline carbon edge of the graphite, called D-band. Graphite dominated porous carbon because of the high G-band value of both carbon electrodes. The ratio of G-band and D-band of two carbon electrodes are 0.45 and 0.48, respectively. The high value of the G-band and D-band ratio means good electroconductivity property. On the other hand, in Fig. 1. (d) was observed the anatase

and rutile composite crystal phase after added into the carbon graphite plate, anatase peak at 2θ value of 47.6°, 53.5° , and 55.1° ; and 2θ values peak of rutile were found at 35.6° and 61.0° , which is coincided with crystal planes of anatase (200), (105), and (211); rutile crystal planes of (101) and (310) [51]. Although graphite carbon plate has good electroconductivity, it has been reported that it is inapplicable for the mediation of water environment due to the hydrophobic property. Thus, anatase and rutile were added into the graphite carbon plate to change the surface of the graphite carbon plate into a hydrophilic property. TiO_2 doped porous carbon plate would be used for water mediation was proposed in this study.

3.3.2 Doping alginate into TiO_2 doped porous carbon plates

Two types of porous carbon plates were cut into a given area (1.0 cm ´ 1.0 cm × 0.2 cm) immersed with 5μM to 750μM of alginate concentration solutions and vacuumized for 120 min using the vacuum pump. And two types of porous carbon electrode weights were measured after drying at 80^{o}C by an oven for 2 h. Figure. 2 (a) shows the weight increased trend of TiO_2 doped porous carbon concerning doping time. It showed that TiO_2 doped porous carbon plate weight became saturation at a low concentration of 21.17 M, 42.34 M, 84.68 M, and 127.02 M alginate in 60 min doping time. However, as the concentrations of alginate solution were increased, carbon plates exhibited the weight increased gradually for 120 min doping process. When the concentration of alginate solution in 0.005 M was doped into TiO_2 doped porous carbon plate for 120 min, the weight increased 0.001 g after oven-dried processes, the ultimate

weight of TiO_2 doped porous carbon was rose to 0.164 g in 254.05 M concentration of alginate solution in 120 min doping process. Therefore, the carbon weights were regularly increased with alginate concentration was increased.

As previously mentioned, TiO_2 doped porous carbon plate has high electroconductivity. Alginate doping afflicting the electroconductibility of TiO_2 doped

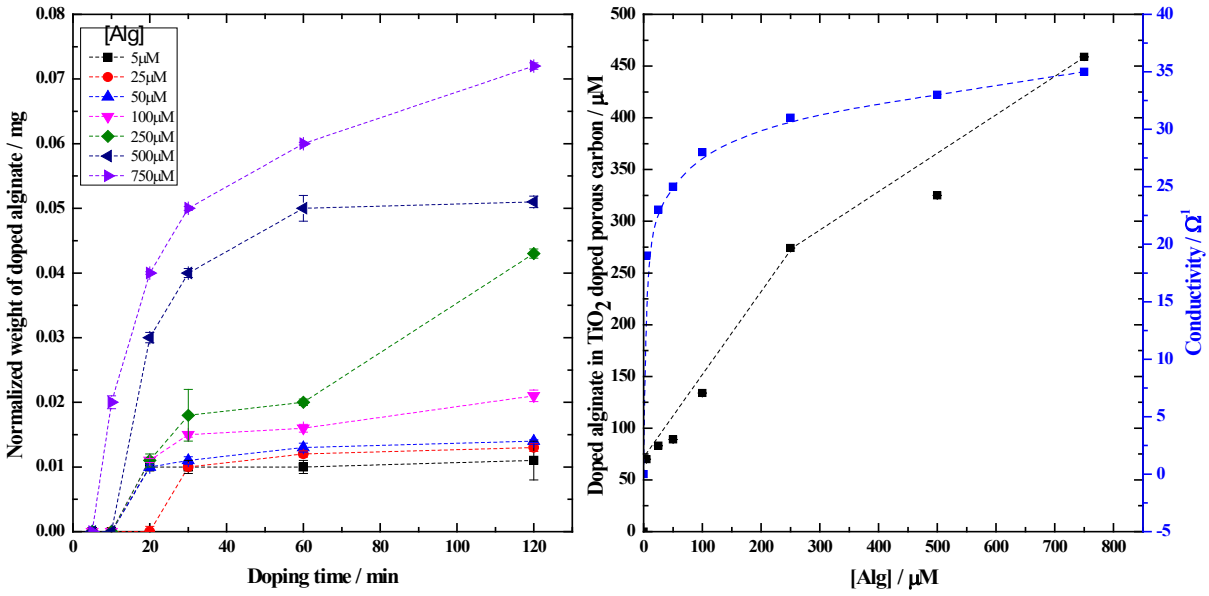

Figure 2. (a) Normalized weight of carbon plate 1 g (1cm ´ 1cm ´ 0.2cm) with doped alginate in 120 min; (b) Conductivity changed with concentration of doped aliginate in TiO_2 doped porous carbon electode plate (1cm ´ 1cm ´ 0.2cm) in 120 min doping process.

porous carbon has to be considered as well. Fig. 2 (b) shows that the electroconductivity of the original TiO_2 doped porous carbon and doped alginate with TiO_2 doped porous carbon. The original average electroconductivity value of the TiO_2 doped porous carbon electrode is 10 Ω^{-1}. As the amount increased alginate intermingled with TiO_2 doped porous carbon, the electroconductivity value was increasing. The concentration of doped alginate exceeded 2.69 M in TiO_2 doped porous carbon, electroconductivity

value has not changed too obviously, but still increased slowly. As the alginate initially was doped inside the porous carbon plates surplus alginate would stick to the surface thereby increasing the electroconductivity of carbon plates.

3.3.3 Sorption isotherm

Sorption isotherms are used to exhibit the adsorbents of how to interact with adsorbate and their distribution on the surface of the adsorbents. It is used to compare the affinity of absorbents for ions of pollutants removal in the hydrosphere as well.

There are several common sorption isotherms already to express the efficiency of adsorbents. However, in this study alginate was doped into the porous carbon plates constitute multilayer absorbent. As a result, a common sorption isotherm could not be used in this study. Here, one new sorption isotherm was discussed based on the Langmuir sorption isotherm. The Langmuir adsorption isotherm is the most common method for describing adsorption capacity, which has been applied to real ions adsorption processes in many studies. It assumes that at first adsorbates are uniformly distributed on a homogeneous monolayer adsorbent [52]. We also assumed that despite inside alginate is the random distribution, the surface of alginate also is a homogeneous monolayer. Therefore, the equation is given as followed:

$$Sr^{2+} + Alg_{site} \leftrightarrows Sr^{2+} - Alg_{site} \quad (1)$$

The $[Sr^{2+}]$ means the free Sr^{2+} concentration reacts with the $[Alg_{site}]$, which means the alginate site. $[Sr^{2+} - Alg_{site}]$ exhibits the concentration of Sr^{2+} combined with

the alginate site. The affinity constant [K] can be written as:

$$K = \frac{[Sr^{2+} - Alg_{site}]}{[Sr^{2+}][Alg_{site}]} \quad (2)$$

The calculation of the concentration of $[Alg_{site}]$ can be simply considered as the maximum adsorption ability $[Alg_{site}]_{max}$ subtracts $[Sr^{2+} - Alg_{site}]$.

$$[Alg_{site}] = [Sr^{2+} - Alg_{site}]_{max} - [Sr^{2+} - Alg_{site}] \quad (3)$$

Eq. (4) is substituted for Eq. (3), and the equation can be rewritten as:

$$\frac{1}{[Sr^{2+} - Alg_{site}]} = \frac{1}{K[Sr^{2+} - Alg_{site}]_{max}} \times \frac{1}{Sr^{2+}} + \frac{1}{[Sr^{2+} - Alg_{site}]_{max}} \quad (4)$$

Here, K and $[Alg_{site}]_{max}$ are affinity of absorbent the maximum sorption capacity. The Sr^{2+} sorption kinetic and sorption isotherm analysis using alginate doped into TiO_2 doped porous carbon plate were described.

3.4 Results and discussion

3.4.1 Sr^{2+} sorption analysis

In this study, a study of Sr^{2+} sorption amount using alginate was conducted to verify Sr^{2+} sorption ability to use alginate. Then, alginate doped inside TiO_2 doped porous carbon with a potential change and without potential change for 120 min process was described. Bulk alginate absorb Sr^{2+} has already been discussed in many other studies [57]. However, there are no same values of the amount and efficiency of Sr^{2+} sorption by using bulk alginate. Therefore, in this article alginate for Sr^{2+} also was conducted

but only as supplement data.

3.4.2 Alginate doped TiO_2 doped porous carbon behavior on Sr^{2+} sorption

Alginate in 254.05 M concentrations showed 68 % and 77.4 % Sr^{2+} sorption in 5 mg/L and 10 mg/L initial Sr^{2+} concentration, respectively. The Sr^{2+} was still approximately left 30 %. Therefore, Sr^{2+} adsorption using alginate still needs to enhance its adsorption amount. As previously mentioned, the electrochemical method was introduced in this study to enhance Sr^{2+} sorption percentage and capacity.

Fig. 3. (a) shows that the Sr^{2+} adsorption of alginate concentrations with TiO_2 doped porous carbon absorbed 57.06 μM and 114.12 μM Sr^{2+} in-circuit closed and open conditions, respectively. The efficiency of complex TiO_2 doped porous carbon is 30 % in 57.06 μM Sr^{2+} sorptions for 120 min sorption processes. Also, only 16 % of Sr^{2+} was absorbed in 114.12 μM initial Sr^{2+} concentration. As the results indicated that alginate indirect contact with Sr^{2+} showed a low efficiency due to TiO_2 doped porous carbon impediment. However, as the initial concentration of Sr^{2+} 57.06 μM and 114.12 μM have double different times, the efficiency of Sr^{2+} showed approximately double times differently. Fig. 3. (b) shows alginate doped into TiO_2 doped porous carbon with a given potential at -0.5 V for Sr^{2+} adsorption. At first, as alginate concentration increased insert carbon, the efficiency was increased to 94%, and 93 % at the concentration of alginate in 0.30 M alginate doped into the carbon. However, alginate in 3.47 M concentration doped into TiO_2 doped porous carbon, the Sr^{2+} adsorption efficiency suddenly decreased to 37.2% and 70.3% at 57.06 μM and 114.12 μM initial Sr^{2+} concentration for 120 min

sorption processes, respectively. Even the sorption efficiency was increased by 64 % compared to in-circuit closed condition, the adsorption efficiency is highly affected by alginate phase, once alginate is stuck to the surface of the carbon plate, Sr^{2+} ions only be absorbed by the surface of alginate and affixed to surface, which caused inside alginate no condition to react with Sr^{2+}. While the comparison result also indicated that ionic migration was increased as charging a potential. $COOH^-$ in alginate bond presents negative charge, thus, a negative potential applied could increase Sr^{2+} ionic moving speed to $COOH^-$. Therefore, Sr^{2+} adsorption using alginate with TiO_2 doped porous carbon does not only depend on the electronic applied but also alginate phase would affect the Sr^{2+} adsorption in-circuit open condition.

3.4.2 Sr^{2+} sorption isotherm of Doped alginate with TiO_2 doped porous carbon

In this study, alginate has been doped into TiO_2 doped porous carbon the concentration of alginate was already set up in constant concentration in each carbon plate. According to the alginate sorption efficiency at a given potential applied, alginate in 0.30 M exhibited the highest efficiency for Sr^{2+} sorption. As a result, in Fig. 3. (c), (d) showed a newly revised sorption isotherm of alginate concentration in 0.3 M with TiO_2 doped porous carbon plate for different Sr^{2+} concentrations with and without charging a potential. The affinity constant *K* and $[Sr^{2+} - Alg_{site}]_{max}$ were calculated in Table 2. The affinity of *K* showed more than double times value at a -0.5 V given potential. The static electricity increased the ionic mobility caused Sr^{2+} could be absorbed inside the porous carbon plate and cut off desorption. And the maximum of

Sr^{2+} sorption showed almost more than seven times higher value in open circuit condition. As previously mentioned, alginate is not merely inside the porous carbon,

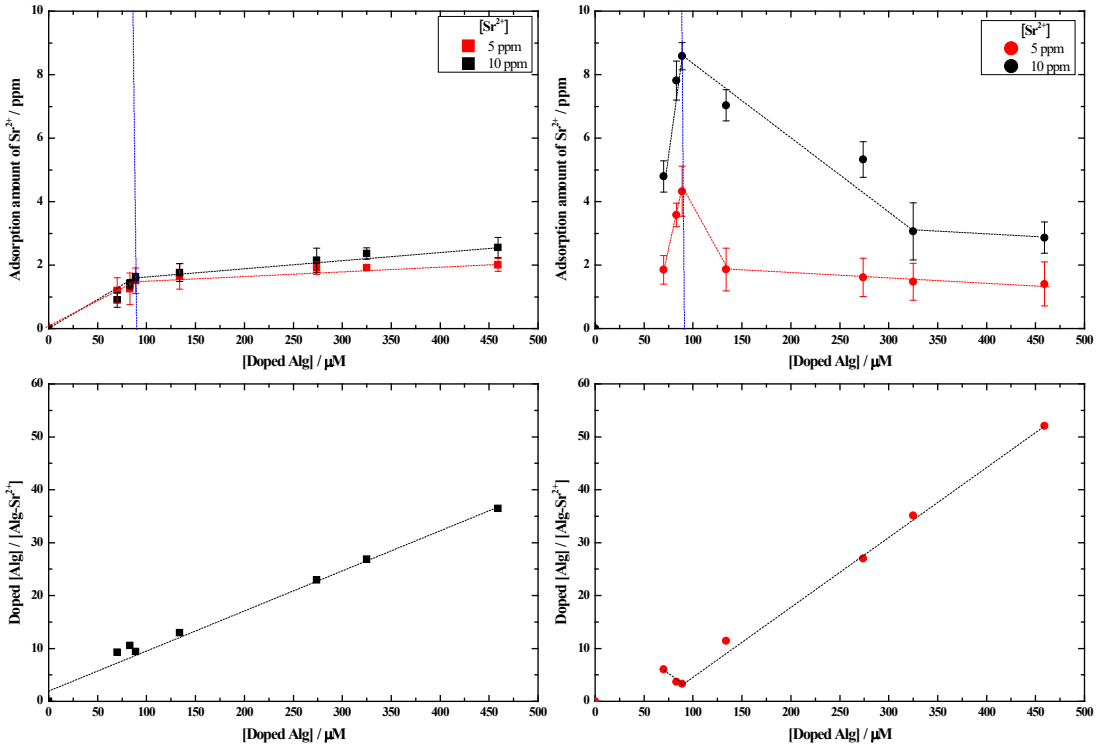

Figure 3. Sr^{2+} adsorption amount using doped alginate with TiO_2 doped porous carbon: (a) without potential; (b) with -0.5 V v.s. Ag/AgCl (sat'd KCl) potential charged in 120 min process. Langumir isotherm of Sr^{2+} adsorption of alginate doped TiO_2 doped porous carbon plate (1cm × 1cm × 0.2cm): (c) without potential; (d) with -0.5 V v.s. Ag/AgCl charge applied in $SrCl_2$ in 120 min process.

the surface of the carbon plate was covered as well. Thus, when applied a negative potential to the carbon plate, the inside alginate first interact with Sr^{2+}, meanwhile, the surface alginate absorbed Sr^{2+} as well.

Table 2 Sr^{2+} adsorption Langmuir isotherm model constants of bulk alginate and doped alginate with TiO_2 doped porous carbon.

Langmuir isotherm			
	K	$[SA]_{max}$	R^2
With potential in $SrCl_2$	0.02	12.61	0.99
Withoout potential in $SrCl_2$	0.03	2.13	0.99
With potential in seawater	0.02	3.30	0.99
Without potential in seawater	0.03	2.08	0.99

3.5 Practical application

Because radionuclides of Sr^{2+} is the final target in this research, the experiment of Sr^{2+} sorption in seawater has to be conducted. Artificial seawater, which is contained approximately 57.06 μM to 114.12 μM of Sr^{2+}, the same concentration as Fukushima harbor seawater is containing. Fig. 4. showed the comparison of doped alginate with TiO_2 doped porous carbon electrode in-circuit closed and circuit open condition of Sr^{2+} sorption amount and efficiency. The doped alginate with the TiO_2 doped porous carbon electrode showed approximately 60 % Sr^{2+} sorption efficiency in -0.5 V given potential. But without the given negative potential, only around 25 % Sr^{2+} was absorbed. Those results are lower than bulk alginate in the $SrCl_2$ experiment. It is owing to artificial seawater containing other substances such as Ca^{2+}, $Mg^{2+,}$ and so on. The alginate absorbs not only strontium but other cations like Ca^{2+}, Mg^{2+} as well [18]. Although the Sr^{2+} sorption amount value is lower than the result value in the $SrCl_2$ solution, the speed of Sr^{2+} amount sorption in the first 5 min is faster than bulk alginate. Therefore, doped

alginate with a TiO_2 doped porous carbon electrode could give a higher Sr^{2+} rate than bulk alginate in-circuit open condition.

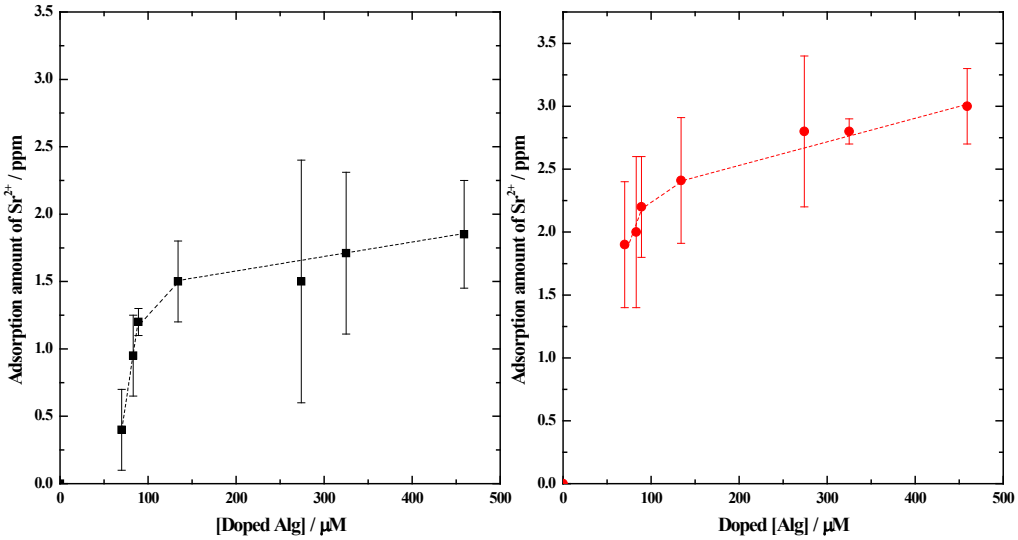

Figure. 4 Adsorption amount of Sr^{2+} by using doped 459 μM alginate with TiO_2 doped porous carbon plate (1cm × 1cm × 0.2cm) : (a) without any potential applied; (b) with -0.5 V v.s. Ag/AgCl (sat'd KCl) potential in 100 ml seawater sample in 120 min Sr^{2+} adsorption process.

According to previous results of Sr^{2+} sorption using alginate with TiO_2 doped porous carbon in seawater. The optimized condition of potential could be controlled in -0.5 V at negative potential and the concentration of alginate could be used in 89 μM. Fig. 5. shows that the area of TiO_2 doped porous carbon was changed and enlarged to 2 cm^2, 3 cm^2, 4 cm^2, and 5 cm^2, respectively. When the area of adsorbents enlarged doped alginate concentration was increased as well. The multiple alginate concentration doped into the TiO_2 doped porous carbon. Meanwhile, the capacity of its sorption efficiency is increased as well. The whole Sr^{2+} was absorbed in 4 cm^2 of the TiO_2 doped porous

carbon with 14.01 M alginate inside. For removing all Sr^{2+} in seawater, doped alginate with TiO_2 doped porous carbon showed more efficiency than bulk alginate. And the amount of alginate utilization is pretty lower than bulk alginate. Hence, doped alginate with enlarged TiO_2 doped porous carbon areas could represent a good behavior for Sr^{2+} sorption in seawater.

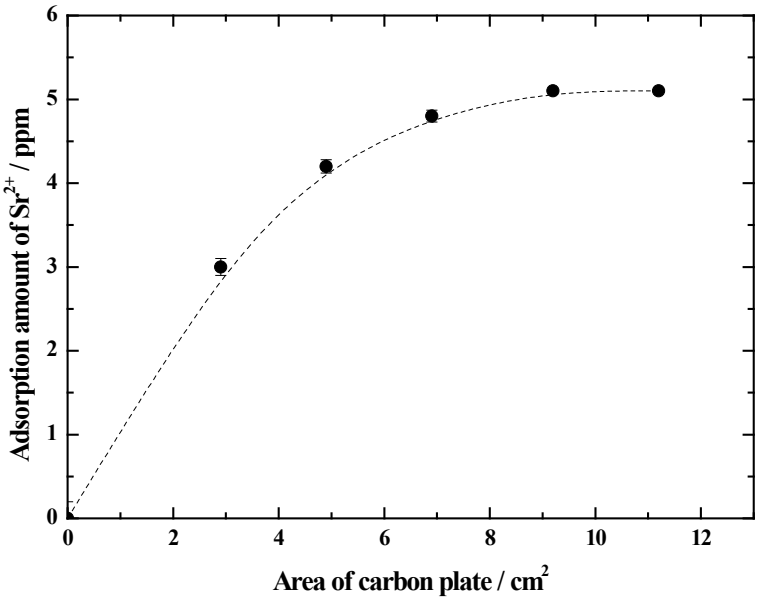

Figure 5. Sr^{2+} adsorption of changing carbon plate areas with doped 459 μM alginate at -0.5 V v.s. Ag / AgCl applied charged in seawater in 120 min absorption process.

Furthermore, Sr^{2+} was absorbed into the carbon plate, it is easy to be treated and safe, such as after burning the carbon plate only Sr^{2+} would be remained and also left Sr^{2+} could be reused as radionuclides energy again. Therefore, this method not only removes Sr^{2+} from the seawater but recycles radionuclides carrier as well.

3.6 Conclusion

Alginate is known as a good adsorbent for the removal of radionuclides, such as Sr^{2+}. However, due to the limited capacity adsorption amounts and other cation ions make compete with Sr^{2+} in seawater, a new adsorbent should be considered.

In this study, the alginate doped into the TiO_2 vacuum impregnated porous carbon electrode to amplify the capacity of Sr^{2+} sorption. The alginate doped TiO_2 doped porous carbon adsorbents performance depends on the initial Sr^{2+} concentration. In solutions containing Sr^{2+} only, alginate doped TiO_2 doped porous carbon adsorbents containing 0.3 M of alginate exhibits the best performance in circuit open condition. Whereas, solutions containing complex mixture matters require more amount of alginate due to the competition of other ions.

Compared to alginate doped TiO_2 doped porous carbon method of Sr^{2+} sorption in -0.5 V potential charged and without the potential for removing Sr^{2+} nearby disaster of Fukushima seawater, doped alginate with TiO_2 doped porous carbon electrode in -0.5 V potential charged could be the best choices.

3.7 References

[1] A. T. Jan, M. Azam, K. Siddiqui, A. Ali, I. Choi, and Q. M. R. Haq, “Heavy metals and human health: Mechanistic insight into toxicity and counter defense system of antioxidants,” *International Journal of Molecular Sciences*. 2015.

[2] J. Suhana and M. Rashid, “Naturally occurring radionuclides in particulate emission from a coal fired power plant: A potential contamination?,” *J. Environ. Chem.*

Eng., 2016.

[3] F. K. Pappa *et al.*, "Radioactivity and metal concentrations in marine sediments associated with mining activities in Ierissos Gulf, North Aegean Sea, Greece," *Appl. Radiat. Isot.*, 2016.

[4] K. Leopold, B. Michalik, and J. Wiegand, "Availability of radium isotopes and heavy metals from scales and tailings of Polish hard coal mining," *J. Environ. Radioact.*, 2007.

[5] M. Villa *et al.*, "Contamination and restoration of an estuary affected by phosphogypsum releases," *Sci. Total Environ.*, 2009.

[6] H. Faghihian, M. Iravani, and M. Moayed, "Application of PAN-NaY Composite for CS+ and SR2+ Adsorption: Kinetic and Thermodynamic Studies," *Environ. Prog. Sustain. Energy*, 2015.

[7] S. Ding, Y. Yang, C. Li, H. Huang, and L. A. Hou, "The effects of organic fouling on the removal of radionuclides by reverse osmosis membranes," *Water Res.*, 2016.

[8] A. Ishag *et al.*, "Environmental application of emerging zero-valent iron-based materials on removal of radionuclides from the wastewater: a review," *Environ. Res.*, 2020.

[9] M. Palamarchuk, A. Egorin, E. Tokar, M. Tutov, D. Marinin, and V. Avramenko, "Decontamination of spent ion-exchangers contaminated with cesium radionuclides using resorcinol-formaldehyde resins," *J. Hazard. Mater.*, 2017.

[10] A. M. El-Kamash, "Evaluation of zeolite A for the sorptive removal of Cs+ and Sr2+ ions from aqueous solutions using batch and fixed bed column operations," *J.*

Hazard. Mater., 2008.

[11] K. M. Abd El-Rahman, A. M. El-Kamash, M. R. El-Sourougy, and N. M. Abdel-Moniem, "Thermodynamic modeling for the removal of Cs+, Sr2+, Ca2+ and Mg2+ ions from aqueous waste solutions using zeolite A," *J. Radioanal. Nucl. Chem.*, 2006.

[12] S. K. Durrani, A. Dyer, and R. Blackburn, "Self-diffusion of barium and caesium cations in neutron- and gamma-irradiated high-silica zeolites and boron-zeotypes," *Zeolites*, 1993.

[13] C. E. Cowan, J. M. Zachara, and C. T. Resch, "Cadmium Adsorption on Iron Oxides in the Presence of Alkaline-Earth Elements," *Environ. Sci. Technol.*, vol. 25, no. 3, pp. 437–446, 1991.

[14] C. L. Thorpe *et al.*, "Strontium sorption and precipitation behaviour during bioreduction in nitrate impacted sediments," *Chem. Geol.*, vol. 306–307, pp. 114–122, 2012.

[15] I. Moreno-Garrido, "Microalgae immobilization: Current techniques and uses," *Bioresour. Technol.*, vol. 99, no. 10, pp. 3949–3964, 2008.

[16] E. Marinho-Soriano, P. C. Fonseca, M. A. A. Carneiro, and W. S. C. Moreira, "Seasonal variation in the chemical composition of two tropical seaweeds," *Bioresour. Technol.*, vol. 97, no. 18, pp. 2402–2406, 2006.

[17] W. A. P. Black, "The seasonal variation in weight and chemical composition of the common British Laminariaceae," *J. Mar. Biol. Assoc. United Kingdom*, vol. 29, no. 1, pp. 45–72, 1950.

[18] S. C. N. Tang, I. M. C. Lo, and M. S. H. Mak, "Comparative study of the adsorption

selectivity of Cr(VI) onto cationic hydrogels with different functional groups," *Water. Air. Soil Pollut.*, 2012.

[19] H. Sone, B. Fugetsu, and S. Tanaka, "Selective elimination of lead(II) ions by alginate/polyurethane composite foams," *J. Hazard. Mater.*, vol. 162, no. 1, pp. 423–429, 2009.

[20] B. An, H. Lee, S. Lee, S. H. Lee, and J. W. Choi, "Determining the selectivity of divalent metal cations for the carboxyl group of alginate hydrogel beads during competitive sorption," *J. Hazard. Mater.*, 2015.

[21] J. S. Rowbotham, P. W. Dyer, H. C. Greenwell, D. Selby, and M. K. Theodorou, "Copper(II)-mediated thermolysis of alginates: a model kinetic study on the influence of metal ions in the thermochemical processing of macroalgae," *Interface Focus*, vol. 3, no. 1, pp. 20120046–20120046, 2012.

[22] J. Burger *et al.*, "Radionuclides in marine fishes and birds from Amchitka and Kiska Islands in the Aleutians: Establishing a baseline," *Health Phys.*, 2007.

[23] S. K. H. Gulrez, S. Al-Assaf, and G. O. Phillips, "Hydrogels : Methods of Preparation , Characterisation and Applications," *Prog. Mol. Environ. Bioeng.*, 2003.

[24] M. Bahram, N. Mohseni, and M. Moghtader, "An Introduction to Hydrogels and Some Recent Applications," in *Emerging Concepts in Analysis and Applications of Hydrogels*, 2016.

[25] D. Song, S. J. Park, H. W. Kang, S. Bin Park, and J. I. Han, "Recovery of lithium(I), strontium(II), and lanthanum(III) using Ca-alginate beads," *J. Chem. Eng. Data*, vol. 58, no. 9, pp. 2455–2464, 2013.

[26] H. J. Hong *et al.*, “Enhanced Sr adsorption performance of MnO2-alginate beads in seawater and evaluation of its mechanism,” *Chem. Eng. J.*, vol. 319, pp. 163–169, 2017.

[27] J. Tang, C. Zhang, X. Shi, J. Sun, and J. A. Cunningham, “Municipal wastewater treatment plants coupled with electrochemical, biological and bio-electrochemical technologies: Opportunities and challenge toward energy self-sufficiency,” *J. Environ. Manage.*, 2019.

[28] F. Geneste, “Catalytic electrochemical pre-treatment for the degradation of persistent organic pollutants,” *Current Opinion in Electrochemistry*. 2018.

[29] C. A. Martínez-Huitle and M. Panizza, “Electrochemical oxidation of organic pollutants for wastewater treatment,” *Current Opinion in Electrochemistry*. 2018.

[30] F. Fu and Q. Wang, “Removal of heavy metal ions from wastewaters: A review,” *J. Environ. Manage.*, vol. 92, no. 3, pp. 407–418, 2011.

[31] A. Jusoh, L. Su Shiung, N. Ali, and M. J. M. M. Noor, “A simulation study of the removal efficiency of granular activated carbon on cadmium and lead,” *Desalination*, vol. 206, no. 1–3, pp. 9–16, 2007.

[32] K. C. Kang, S. S. Kim, J. W. Choi, and S. H. Kwon, “Sorption of Cu2+ and Cd2+ onto acid- and base-pretreated granular activated carbon and activated carbon fiber samples,” *J. Ind. Eng. Chem.*, vol. 14, no. 1, pp. 131–135, 2008.

[33] F. Fu and Q. Wang, “Removal of heavy metal ions from wastewaters: A review,” *J. Environ. Manage.*, vol. 92, no. 3, pp. 407–418, 2011.

[34] A. Nasrullah, A. H. Bhat, A. Naeem, M. H. Isa, and M. Danish, “High surface area

mesoporous activated carbon-alginate beads for efficient removal of methylene blue," *Int. J. Biol. Macromol.*, vol. 107, pp. 1792–1799, 2018.

[35] S. Ravulapalli and K. Ravindhranath, "Removal of lead (II) from wastewater using active carbon of Caryota urens seeds and its embedded calcium alginate beads as adsorbents," *J. Environ. Chem. Eng.*, 2018.

[36] A. S. Rathore, A. Gutman, Electrokinetic phenomena: Principels and applications in analytical chemisty and microchip technology, Dekker, New York, 2004.

[37] H. Ohshima, "Gel electrophoresis of a soft particle," *Advances in Colloid and Interface Science*. 2019.

[38] L. Mendoza, T. Gunawardhana, W. Batchelor, and G. Garnier, "Nanocellulose for gel electrophoresis," *J. Colloid Interface Sci.*, 2019.

[39] B. J. Cha *et al.*, "Photo-catalytic activity of hydrophilic-modified TiO2 for the decomposition of methylene blue and phenol," *Curr. Appl. Phys.*, 2017.

[40] J. F. Cardenas, H. Fredriksson, B. Kasemo, and D. Chakarov, "Light induced selective heating of nanostructured pyrolitic graphite surfaces investigated by Raman scattering," *Chem. Phys.*, 2013.

[41] I. Langmuir, "Adsorption of gases on plain surfaces of glass mica platinum," *J. Am. Chem. Soc.*, 1918.

Chapter 4

Development of Absorbent Using Amylose-Graphite Composite Electrode for Removal of Heavy Metals

Chapter 4: Development of Absorbent Using Amylose-Graphite Composite Electrode for Removal of Heavy Metals

4.1 Introduction

Rising population, factory expansion, urbanization, agricultural activities, and various chemicals usage have led to serious environmental issues [1,2]. Water contamination is the most important of these environmental issues to examine, as water quality has a direct link to human health, as hazardous substances are absorbed in bodily organisms through the food chain and drinking water [1]. Copper, chromium, cadmium, and lead are the most common heavy metal contaminants in Japan. Heavy metals are highly toxic, non-biodegradable, and easily accumulate in human organs, causing various diseases and health disorders [3–6]. After the investigation, it was discovered that the high concentration of copper discharged into the river and infiltrated into the surface of the soil due to copper mining in the Ashio Copper Mine upstream of the Watarase River killed numerous crops and fish died downstream of the Watarase River in Japan in 1890 [7]. In 1905, the Japanese government decided to build sedimentation ponds to remove the mining poison. *Phragmites australis* was planted in large quantities surrounded Watarase River to absorb harmful heavy metals from the water [8]. *Phragmites australis* is still used today to protect water safety and wildlife [7]. Heavy metal contamination in water bodies has resulted in numerous illnesses, such as ITAI-ITAI disease, lead poisoning, and skin fester [9]. Thus, regarding these illnesses, WHO stipulates the standard for different types of heavy metals in water bodies: the copper concentration should be less than 2 mg/L, chromium is set at 0.05 mg/L, cadmium must be less than 0.003 mg/L, and lead must be maintained below 0.01 mg/L

[10]. In addition to complying with regulations, water treatment technology must be implemented to achieve water recycling.

Coagulation, chemical precipitation, oxidation, reverse osmosis, membranes, solid-phase extraction, electrochemical, and adsorption are some of the wastewater treatment technologies developed over the last few decades [11–13]. These technologies have some limitations; for example, chemical precipitation generates sludge, which needs further treatment and will eventually increase the cost [14–16]. Adsorption is the most widely used and recommended method for water treatment due to the adsorbent materials being possible to extract from natural resources, having a large quantity, being easily degradable, having the benefit of being highly efficient, and being less likely to cause secondary pollution to the environment [17–19]. Many materials are used as adsorbent materials for water treatment, such as zeolites, resins, polymeric membranes, and clays that can adsorb heavy metals [20,21]. However, some adsorbent materials showed limited capacity due to adsorption limitations, therefore many researchers are looking for various potential methods such as a modification to enlarge the capacity site [22–24].

Starch is a polysaccharide substance found in enormous quantities in nature, that is inexpensive, biocompatible, renewable, and degradable [25,26]. Amylose and amylopectin are two forms of semi-crystalline granules found in starch [27]. Amylose is less polymerized and has a higher water solubility than amylopectin. The focus of this study is on amylose as an adsorbent material in polymeric membranes. However, existing natural starch is not easily soluble in water; thus, changing the chemical and physical properties has become an approach for its wide use [28]. Most studies have demonstrated that modifying starch could change its response to pH value and temperature limitation [29,30]. There is also the possibility of adding specific

functional groups to starch, such as amino, hydroxyl, and carboxyl groups to improve the adsorption affinity for heavy metal ions in water treatment. Various studies have succeeded in replacing the hydroxyl group of starch with different groups, such as carboxyl and acetyl group insertion [31]. There are many approaches to chemically altering starch like acid hydrolysis, cross-linking, and oxidation to replace the hydroxyl groups [32,33]. However, the hydroxyl group on the backbone of starch is one of the beneficial functional groups for heavy metal adsorption, and modifying its chemical properties does not essentially increase its adsorption surface area.

Therefore, in this study, we propose a new concept in which we use amylose in starch as a basic absorbent and then add carboxyl functional groups at the periphery interface to increase its absorption surface area using the electrochemical driving force. Carbon materials are well known for having carboxyl functional groups surrounded by the backbone, low cost, and environmental friendliness, so they have become one of the common adsorbent materials [34,35]. Activated carbon is used as one of the common adsorbent materials because of its high surface area. However, it gradually loses its adsorption efficiency due to the limited sorption site [36]. Gang X. et al. suggested that graphitic carbon nitride nanosheets can adsorb cationic and anionic ions in wastewater because of the absorbents' special shape and semi-conductivity properties [37]. Many studies have shown that the carbon materials are used as adsorbent materials; the pH value in the water body needs to be changed in most cases because the carboxyl groups are easily affected by different pH values [38,39]. Therefore, an adsorbent material that is not affected by the pH but has high absorption ability is requested.

We believe that a composite of graphite and starch amylose could be a new heavy metal absorption material in wastewater treatment. Different amylose concentrations

were used to modify the graphite carbon plates to analyze the absorption efficiency hoping to find the optimized concentration of amylose usage. Then, the material was conducted with a negative charge to calculate the absorption efficiency and compared with the results of uncharged experiments to confirm if the efficiency was improved. We expected the new absorption material to absorb various heavy metal ions from contaminated water efficiently and quickly.

4.2 Materials and Methods

4.2.1 Materials

All reagents used in this study were analytical grade. Standard solutions of copper (II) chloride, lead (II) chloride, cadmium (II) chloride, chromium (VI) oxide, potassium chloride, and amylose of starch were purchased from Wako, Japan. Potassium chloride was added as an electrolyte when the electrochemical method was applied. Hitachi Chemical Co., Ltd. donated porous carbon plates.

4.2.2 Instruments

In this study, the characterization of graphite porous carbon plates was measured using Scanning Electrode Microscopy (SEM, Hitachi, S4800 series), X-ray diffraction (XRD, RINT2200V), Raman spectroscopy (JASCO, RMP 500), and a digital multimeter (ADVANTEST, R6450). The amylose and graphite porous carbon plate was used in the vacuum system and new adsorbent materials were dried in an oven at 80 °C. The adsorption of heavy metals was performed using an Electrochemical Instrument (HOKUTO DENKO, HZ-7000), with three electrodes connected. The working electrode (WE), counter electrode (CE), and reference electrode (RE) were amylose/graphite porous carbon plate,/graphite porous carbon plate, and Ag/AgCl

electrode, respectively. The concentration of heavy metal ions was measured using an Atomic Absorption Spectrophotometer (AAS, Hitachi Z-2000).

4.2.3 Characterization of Graphite Porous Carbon Plate

Two types of graphite carbon plate could be a potential material. Two types of graphite porous carbon plates were prepared; SEM was used to observe the appropriate porous size, for which samples were controlled in magnification: 4000, working distance: 17.4 mm, acceleration voltage: 5 KV, and emission current: 10 μA condition. SEM images (Figure 1a,b) show the pore size of the two types of graphite porous carbon plate; the cavity of the pore was measured at 5 μm. According to the SEM images, two graphite porous carbon plate exposed a similar pore size, and the multilayer sheets were also expressed.

However, XRD was used to identify the carbon components and detect the carbon crystal phase of two porous carbon plates using Cu-Ka radiation of 1.5405 Å wavelength and a scanning speed of 2° min^{-1}. The surface property of porous carbon electrodes was investigated using Raman spectroscopy (JASCO, RMP 500). In carbon materials, Raman spectroscopy is used to detect bond strengths via lattice vibration. Figure 1cd shows the XRD and Raman spectra of two types of porous carbon plates. As a result, two types of porous carbon showed a typical graphite peak in XRD patterns at $2\theta = 26.7°$ [40]. In Raman spectra, the main features of the G-band and D-band appear at 1582 cm^{-1} and 1350 cm^{-1}, respectively. The Raman peak around 1582 cm^{-1} is known as the G-band typical Raman peak of bulk crystalline graphite. This peak is the basic vibration mode of graphite crystals. The size of the crystal influences the intensity [41]. The vibration of the crystalline carbon edge of the graphite, known as the D-band, produces a peak value of 1350 cm^{-1}.

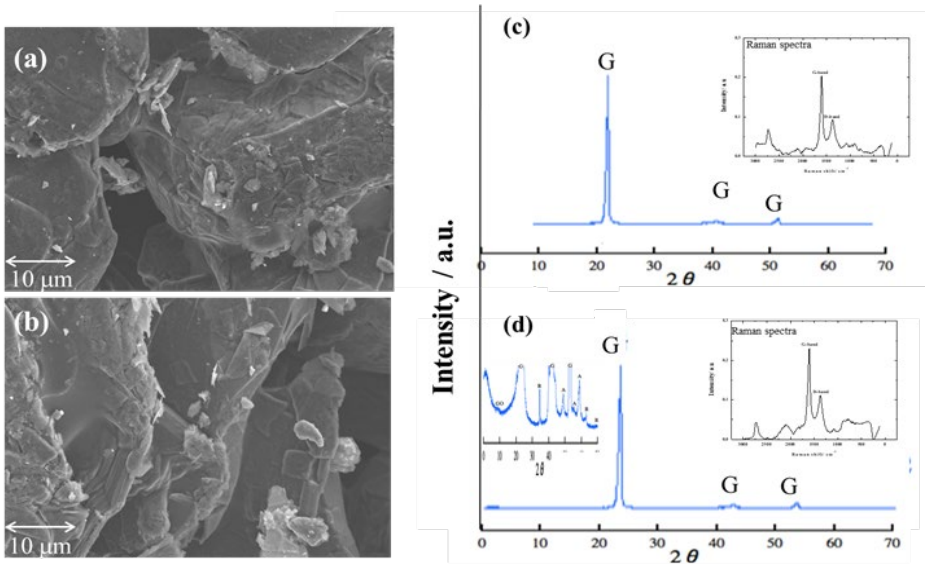

Figure 1. SEM imagines of (**a**) porous carbon; (**b**) TiO_2-doped graphite porous carbon. (I: 10 μA V:5 kV Mag: 4000 WD: 17.4 mm). XRD and Raman spectra of (**c**) porous carbon; (**d**) TiO_2-doped graphite porous carbon.

Regarding the Raman spectra, graphite-dominated porous carbon was noticed because the high G-band value was exposed in both carbon electrodes. The high value of the G-band and D-band ratio means good electroconductivity property [42]. The ratio of G-band and D-band of two carbon electrodes were 0.45 and 0.48, respectively. Furthermore, anatase and rutile composite crystal phases were observed in Figure 1d after being added to the carbon graphite plate with anatase peaking at 2θ values of 47.6°, 53.5°, and 55.1°; and 2θ values peak of rutile were found at 35.6° and 61.0°, which coincided with crystal planes of anatase (200), (105), and (211), and rutile crystal planes of (101) and (310) [43]. Graphite carbon plates have good electroconductivity, but their hydrophobic characteristic makes them unsuitable for water mediation. Thus, anatase and rutile were added to the graphite carbon plate to change the surface of the graphite

carbon plate for a hydrophilic property. TiO_2-doped graphite porous carbon plate was used as a potential material for water mediation in this study.

4.2.4 Doping Amylose into Graphite Porous Carbon Plates

The vacuum pump was used to vacuumize TiO_2-doped graphite porous carbon plates, which were subsequently immersed in 10g of amylose solutions and vacuumed for 120 min. The weights of amylose / TiO_2 doped porous carbon plates were measured after they were removed from the solution and dried in an oven at 80 °C for 120 min. Figure 2 shows the dried weight of amylose / TiO_2-doped porous carbon increased tendency. It shows that the weight of TiO_2 - doped porous carbon plate became saturated in 120 min of doping time. The lowest carbon area (1.0 cm × 1.0 cm × 0.2 cm) showed 0.1 g change and the biggest carbon plate area (9.0 cm × 15.0 cm × 0.2 cm) showed 0.9 g change; thus, the amylose of starch increased proportionally with the carbon plate area. Since the electrochemical method was to be used, the area of carbon plate was chosen to be 5.0 cm × 9.0 cm × 0.2 cm for ease of operation.

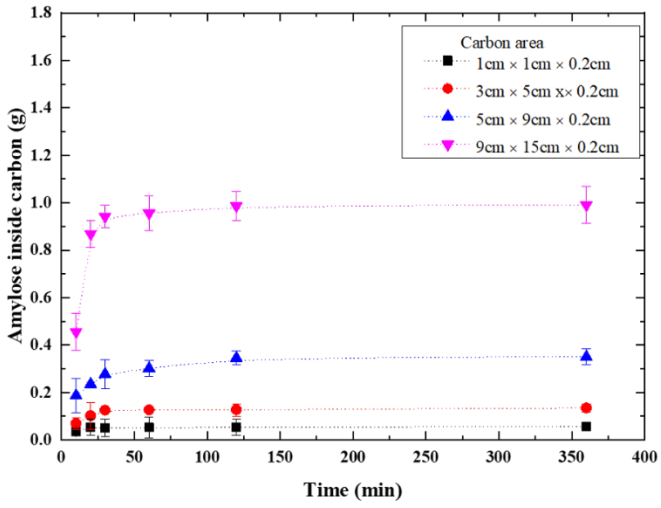

Figure 2. Time dependence of amylose doped into TiO_2-doped graphite porous carbon.

4.2.5 Absorption Isotherm

Absorption isotherms show how the absorbents interact with adsorbate and their distribution on the surface. It has also been used to compare the affinity of absorbents for removing contaminants from the hydrosphere.

The Langmuir isotherm is the most common method for describing the absorption capacity, applied to real ions absorption processes in many studies. There are already several common isotherms to express the efficiency of adsorbents. However, in this study, amylose was doped into the graphite multilayer sheet plate; the common adsorption isotherm could not certainly be consistent in this study. Here, one new absorption isotherm was discussed based on the Langmuir sorption isotherm. It assumes that at first, adsorbates are uniformly distributed on a homogeneous monolayer absorbent. We also assumed that despite inside amylose being random distribution, the surface of amylose also shows a homogeneous monolayer. Therefore, the equation is given as follows:

$$HM^{2+} + A_{site} \leftrightarrows HM^{2+} - A_{site} \quad (1)$$

$[HM^{2+}]$ means the free concentration of heavy metal ions in solution, $[A_{site}]$ means the amylose absorption site. $[HM^{2+} - A_{site}]$ exhibits the absorbed concentration of heavy metals in the new absorbent. Regarding the chemical equilibrium reaction, the affinity constant $[K]$ can be written as follows:

$$K = \frac{[HM^{2+} - A_{site}]}{[HM^{2+}][A_{site}]} \quad (2)$$

The calculation of the concentration of $[A_{site}]$ can simply be considered the maximum absorption ability of $[A_{site}]$ subtraction.

$$[A_{site}] = [HM^{2+} - A_{site}]_{max} - [HM^{2+} - A_{site}] \quad (3)$$

Equation (4) is substituted from Equation (3), and the equation can be rewritten as follows:

$$\frac{1}{[HM^{2+}-A_{site}]}=\frac{1}{K[HM^{2+}-A_{site}]_{max}}\times\frac{1}{A_{site}}+\frac{1}{[Heavy\ metal^{2+}-Amylose_{site}]_{max}} \quad (4)$$

Here, K and $[A_{site}]_{max}$ exhibit affinity of absorbent and the maximum absorption capacity, respectively. The heavy metal absorption isotherm analysis using amylose doped into graphite porous carbon electrode was described.

4.3 Results

4.3.1 Heavy Metal Absorption Amount Analysis

This study on heavy metal ion absorption amount using amylose was conducted to verify heavy metal ion absorption ability. Then, the amylose/TiO_2-doped graphite porous carbon was described at a given potential change for a 120 min heavy metal ion absorption process. Figure 3a shows the absorption amount of Pb^{2+} using amylose/TiO_2-doped graphite porous carbon in 0.3 g at a −0.5 V charged potential applied. The absorption amount is 66.11 mg/L; approximately 26.4% of Pb^{2+} had been absorbed at the end of 120 min. However, at the initial concentration, 100 mg/L of Pb^{2+} exposed to approximately 47.52% of Pb^{2+} was absorbed in 120 min. According to the absorption rate for lead removal, 100 mg/L could be a critical initial concentration for the absorption equilibrium. Figure 3b shows the maximum absorption amount of 57.69 mg/L for 250 mg/L Cu^{2+} absorptions using amylose/TiO_2-doped graphite porous carbon in 0.3 g at a −0.5 V charged potential applied; however, the capacity of absorption in Cu^{2+} solution showed 40.76% at the initial 100 mg/Lof Cu^{2+}. As a result, the absorption amount of the developed absorbent has the best absorption performance at 100 mg/L of Cu^{2+}. Figure 3c shows the absorption amount of Cd^{2+}, and the results show that even though absorption

amount continued to grow as cadmium concentration increased, the absorption amount decreased over 200 mg/L of Cd^{2+} absorption, which is a similar phenomenon to Pb^{2+} and Cu^{2+}. The maximum absorption amount and capacity were 47.81 mg/L and 42.65%, respectively. Cr^{6+} absorption amount is also described in Figure 3d, which shows the lowest absorption amount among these heavy metals. The maximum absorption amount value was shown at 39.68 mg/L for an initial concentration of 150 mg/L Cr^{6+} absorption, and the maximum absorption capacity appeared on the 100 mg/L, which showed approximately 34.68% absorption capacity. The maximum absorption amount and capacity are summarized in Table 1. Amylose/TiO_2-doped graphite porous carbon for

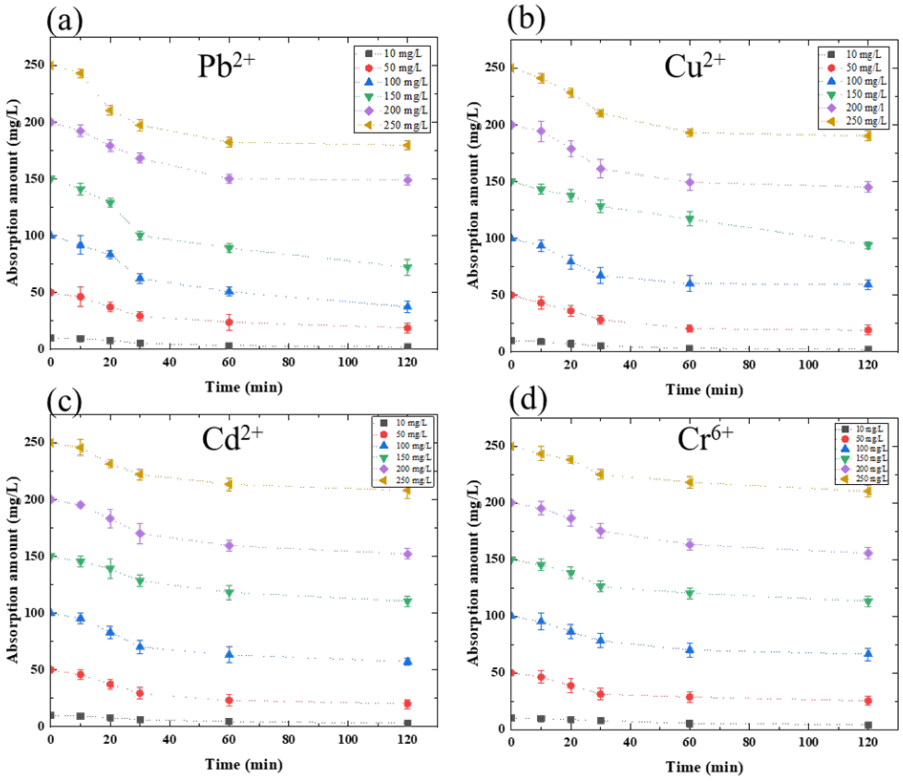

Figure 3. Absorption amount in different heavy metal concentration solutions: (**a**) Pb^{2+}; (**b**) Cu^{2+}; (**c**) Cd^{2+}; (**d**) Cr^{6+} using 0.3 g amylose/TiO_2-doped graphite porous carbon at −0.5 V potential.

removal of heavy metals exhibited the best absorption amount at the initial concentration of 100 mg/L individually, but it showed a different value of absorption amount and

capacity. The size of the ionic radius of Pb^{2+}, Cu^{2+}, Cd^{2+}, and Cr^{6+} is 1.75 Å, 1.28 Å, 1.49 Å, and 1.25 Å, respectively. The size of heavy metal ions determined the absorption ability and the absorption affinity.

Table 1. The absorption amount and capacity for each heavy metal removal by using 0.3 g amylose/TiO_2-doped graphite porous carbon at −0.5 V potential.

	Pb^{2+}	**Cu^{2+}**	**Cd^{2+}**	**Cr^{6+}**
Absorption amount (mg L^{-1})	66.11	57.69	47.81	39.68
Maximum absorption capacity (%)	47.52	40.76	42.65	34.68

4.3.2 Heavy Metal Absorption Isotherm of Amylose/TiO_2 Doped Graphite Porous Carbon

In this study, amylose was fixed at a certain amount into TiO_2-doped graphite porous carbon in each plate. To understand the absorption rate and how the electrochemical driving force method works for the removal of heavy metals, the affinity constant K and $[HM^{2+} - A_{site}]_{max}$ were calculated in Table 2 based on the established absorption isotherm. The new absorbent order of each heavy metal's absorption ability is as follows: Cu^{2+} > Pb^{2+} > Cr^{6+} > Cd^{2+}. The value of maximum absorption amount calculated from the absorption isotherms is similar to the results appeared in the experiments, the absorption amount of Cu^{2+} and Pb^{2+}, and Cr^{6+} and Cd^{2+} were approximately at the same value. It is inferred that the ionic radius of Cu^{2+} and Pb^{2+} are close; Cr^{6+} and Cd^{2+} are at a similar value as well. Since the maximum absorption amount of the single component amylose absorbent showed that Pb^{2+}(20.89-mg/L) > Cu^{2+} (19.15-mg/L) > Cd^{2+} (15.86-mg/L) > Cr^{6+} (13.29-mg L), the amylose-doped TiO_2-doped graphite porous carbon absorbent had a higher absorption ability than the single component amylose absorbent.

Figure 4 showed that even if all of the heavy metal concentrations could not pass through the linear lines for every single point, most points are on the line. Therefore, the new absorbent could fix this new absorption isotherm. As previously mentioned, amylose does not show a homogeneous distribution on the surface of TiO_2-doped graphite porous carbon. First, potential charges occurred with amylose covered by the carbon plate's surface; subsequently, inside amylose acted as the charge potential continued.

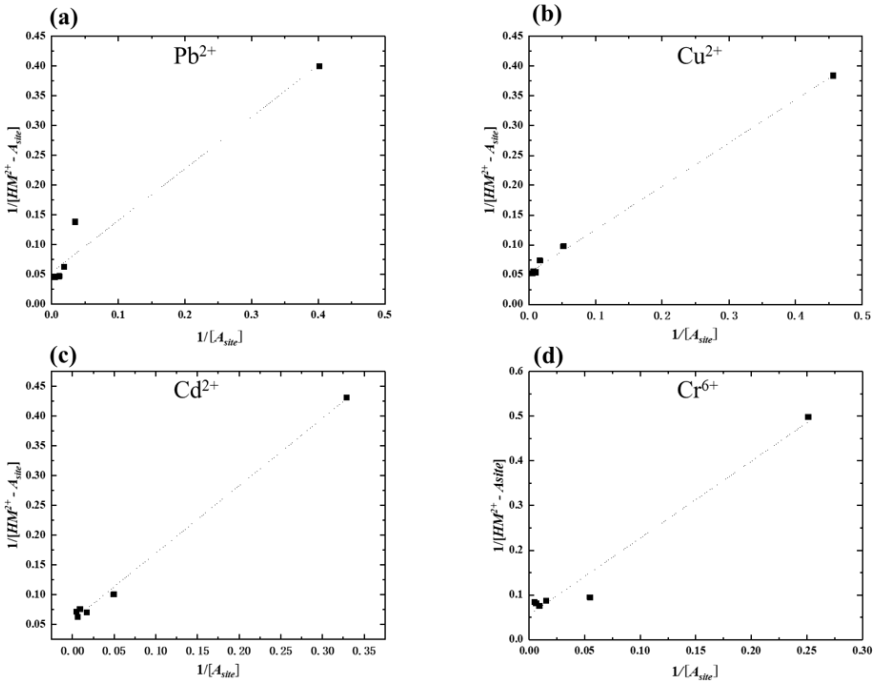

Figure 4. The absorption isotherm fitting for each heavy metal absorption: (**a**) Pb^{2+}; (**b**) Cu^{2+}; (**c**) Cd^{2+}; (**d**) Cr^{6+} using 0.3 g amylose/TiO_2-doped graphite porous carbon at −0.5 V potential.

Table 2. The maximum absorption amount and affinity for each heavy metal absorption by using 0.3 g amylose/TiO_2-doped graphite porous carbon at −0.5 V potential.

	Pb^{2+}	**Cu^{2+}**	**Cd^{2+}**	**Cr^{6+}**
Maximum absorption amount (mg/L)	55.89	56.82	52.83	53.97
K	0.06	0.07	0.05	0.03

4.3.3 Practical Application

As is well known, heavy metals contaminated with water have frequently co-existed with multi-species. The absorption of heavy metals in mixed water samples was investigated. Each heavy metal's initial concentration ranged from 10 mg/L to 250 mg/L. The amount of absorbent was charged with the same potential as the individual experiment. Figure 5 shows each heavy metal absorption amount for 120 min absorption progress in a mixed solution. The absorption capacities for heavy metal removal are exhibited differently from a single ion absorption. The maximum absorption capacities occurred in the initial concentration of 100 mg/L of each ion, as

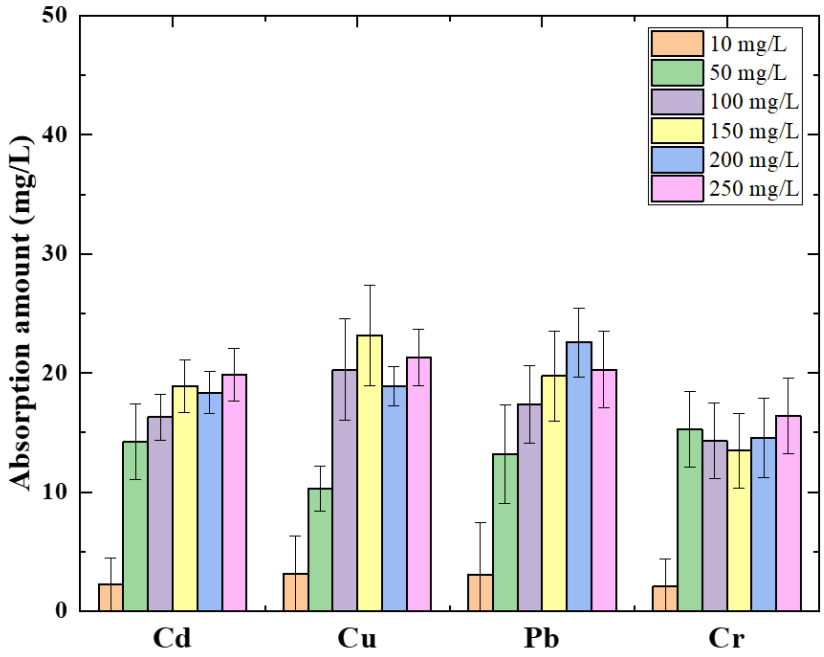

Figure 5. Absorption amount in different commixture of heavy metals concentration solutions using 0.3 g amylose/TiO_2-graphite porous carbon at −0.5 V potential.

with the individual heavy metal absorption results. The average of mixed heavy metal absorption was 21.46 mg/L. The maximum absorption amount value is shown in Table 3 for each heavy metal absorption based on the absorption isotherm. The order of maximum absorption for mixed heavy metals is Cd^{2+} > Cr^{6+} > Pb^{2+} > Cu^{2+}. The

maximum absorption amountsdeclined, and the order of the value expressed the opposite to the individual absorption value. However, this result can be considered to follow the ionic radius as well.

Table 3. The maximum absorption amount and affinity for mixed heavy metal absorption using 0.3 g amylose/TiO_2-graphite porous carbon at −0.5 V potential.

	Pb^{2+}	**Cu^{2+}**	**Cd^{2+}**	**Cr^{6+}**
Maximum absorption amount (mg/L)	30.21	27.75	44.31	32.31
K	0.017	0.019	0.007	0.009

In the mixed solution, amylose on the surface absorbed the smaller size of ions making the inside of amylose unavailable for work, resulting in a two-fold decrease in average absorption levels. Despite an absorption competition in mixed solutions, the absorption amount is still as good as expected.

4.4 Conclusion

The electrochemical driving force approach was used to test a new absorbent using an amylose/TiO_2-doped graphite porous carbon electrode for heavy metal absorption in this study. The performance of amylose-doped TiO_2-doped graphite porous carbon absorption depended on the initial concentration of heavy metals, and the absorption equilibrium concentration was 100 mg/L. It was shown that the absorption amount and ability were advanced for single component amylose absorbent and single heavy metal absorption. Meanwhile, the devised absorption isotherm is in accordance with the absorption trend of the new absorbent material for heavy metals absorption, and the ionic radius determined the order of heavy metal maximum absorption. There is an opposite order compared to one heavy metal ion and mixed solution. In contrast, the electrochemical driving fore method for compositing porous carbon plate and amylose could drastically improve the absorbent ability compared to bulk amylose application.

4.5 References

[1] P. A. S. S. Marques, M. F. Rosa, and H. M. Pinheiro, “pH effects on the removal of Cu2+, Cd2+ and Pb2+ from aqueous solution by waste brewery biomass,” *Bioprocess Eng.*, vol. 23, no. 2, pp. 135–141, 2000, doi: 10.1007/PL00009118.

[2] F. Zahir, S. J. Rizwi, S. K. Haq, and R. H. Khan, “Low dose mercury toxicity and human health,” *Environ. Toxicol. Pharmacol.*, vol. 20, no. 2, pp. 351–360, 2005, doi: 10.1016/j.etap.2005.03.007.

[3] T. Zhang *et al.*, “Removal of heavy metals and dyes by clay-based adsorbents: From natural clays to 1D and 2D nano-composites,” *Chem. Eng. J.*, vol. 420, no. P2, p. 127574, 2021, doi: 10.1016/j.cej.2020.127574.

[4] K. Khoeurn, A. Sakaguchi, S. Tomiyama, and T. Igarashi, “Long-term acid generation and heavy metal leaching from the tailings of Shimokawa mine, Hokkaido, Japan: Column study under natural condition,” *J. Geochemical Explor.*, vol. 201, no. November 2018, pp. 1–12, 2019, doi: 10.1016/j.gexplo.2019.03.003.

[5] G. Yan and T. Viraraghavan, “Heavy metal removal in a biosorption column by immobilized M. rouxii biomass,” *Bioresour. Technol.*, vol. 78, no. 3, pp. 243–249, 2001, doi: 10.1016/S0960-8524(01)00020-7.

[6] T. Makino, S. Ishikawa, M. Murakami, and T. Arao, “Spatial Distribution and

Risk Management of Heavy Metal Contamination in Japan," no. 2001, pp. 3–5, 2014.

[7] D. Magee, "Brett L. Walker, Toxic archipelago: A history of industrial disease in Japan (Seattle: University of Washington Press, 2010)," *J. Environ. Stud. Sci.*, vol. 1, no. 2, pp. 156–158, 2011, doi: 10.1007/s13412-011-0021-4.

[8] Conley, "The World Whole : An Environmental History of Japanese Space Power," vol. 1973, pp. 1–265, 2014.

[9] T. Inaba *et al.*, "Estimation of cumulative cadmium intake causing Itai-itai disease," *Toxicol. Lett.*, vol. 159, no. 2, pp. 192–201, 2005, doi: 10.1016/j.toxlet.2005.05.011.

[10] Y. Sayato, "WHO Guidelines for Drinking-Water Quality," *Eisei kagaku*, vol. 35, no. 5, pp. 307–312, 1989, doi: 10.1248/jhs1956.35.307.

[11] Y. Sun, S. Zhou, S. Y. Pan, S. Zhu, Y. Yu, and H. Zheng, "Performance evaluation and optimization of flocculation process for removing heavy metal," *Chem. Eng. J.*, vol. 385, no. October 2019, p. 123911, 2020, doi: 10.1016/j.cej.2019.123911.

[12] N. Meunier, P. Drogui, C. Montané, R. Hausler, J.-F. Blais, and G. Mercier, "Heavy Metals Removal from Acidic and Saline Soil Leachate Using Either Electrochemical Coagulation or Chemical Precipitation," *J. Environ. Eng.*, vol. 132, no. 5, pp. 545–554, 2006, doi: 10.1061/(asce)0733-9372(2006)132:5(545).

[13] R. Shrestha *et al.*, "Technological trends in heavy metals removal from industrial wastewater: A review," *J. Environ. Chem. Eng.*, vol. 9, no. 4, p.

105688, 2021, doi: 10.1016/j.jece.2021.105688.

[14] D. T. Sun *et al.*, “Rapid, Selective Heavy Metal Removal from Water by a Metal-Organic Framework/Polydopamine Composite,” *ACS Cent. Sci.*, vol. 4, no. 3, pp. 349–356, Mar. 2018, doi: 10.1021/acscentsci.7b00605.

[15] J. He *et al.*, “Pyrolysis of heavy metal contaminated Avicennia marina biomass from phytoremediation: Characterisation of biomass and pyrolysis products,” *J. Clean. Prod.*, vol. 234, pp. 1235–1245, Oct. 2019, doi: 10.1016/J.JCLEPRO.2019.06.285.

[16] C. Duan, T. Ma, J. Wang, and Y. Zhou, “Removal of heavy metals from aqueous solution using carbon-based adsorbents: A review,” *J. Water Process Eng.*, vol. 37, p. 101339, Oct. 2020, doi: 10.1016/J.JWPE.2020.101339.

[17] Á. García-Padilla, K. A. Moreno-Sader, Á. Realpe, M. Acevedo-Morantes, and J. B. P. Soares, “Evaluation of adsorption capacities of nanocomposites prepared from bean starch and montmorillonite,” *Sustain. Chem. Pharm.*, vol. 17, p. 100292, Sep. 2020, doi: 10.1016/J.SCP.2020.100292.

[18] L. Guo *et al.*, “Porous starches modified with double enzymes: Structure and adsorption properties,” *Int. J. Biol. Macromol.*, vol. 164, pp. 1758–1765, Dec. 2020, doi: 10.1016/J.IJBIOMAC.2020.07.323.

[19] B. M. Ibrahim and N. A. Fakhre, “Crown ether modification of starch for adsorption of heavy metals from synthetic wastewater,” *Int. J. Biol. Macromol.*, vol. 123, pp. 70–80, Feb. 2019, doi: 10.1016/J.IJBIOMAC.2018.11.058.

[20] A. M. Atta, H. A. Al-Lohedan, Z. A. ALOthman, A. A. Abdel-Khalek, and A.

M. Tawfeek, “Characterization of reactive amphiphilic montmorillonite nanogels and its application for removal of toxic cationic dye and heavy metals water pollutants,” *J. Ind. Eng. Chem.*, vol. 31, pp. 374–384, Nov. 2015, doi: 10.1016/J.JIEC.2015.07.012.

[21] M. Tabatabaei Shirazani, H. Bakhshi, A. Rashidi, and M. Taghizadeh, “Starch-based activated carbon micro-spheres for adsorption of methane with superior performance in ANG technology,” *J. Environ. Chem. Eng.*, vol. 8, no. 4, p. 103910, Aug. 2020, doi: 10.1016/J.JECE.2020.103910.

[22] P. Li, B. Gao, A. Li, and H. Yang, “Evaluation of the selective adsorption of silica-sand/anionized-starch composite for removal of dyes and Cupper(II) from their aqueous mixtures,” *Int. J. Biol. Macromol.*, vol. 149, pp. 1285–1293, Apr. 2020, doi: 10.1016/J.IJBIOMAC.2020.02.047.

[23] K. Woo and P. A. Seib, “Cross-linking of wheat starch and hydroxypropylated wheat starch in alkaline slurry with sodium trimetaphosphate,” *Carbohydr. Polym.*, vol. 33, no. 4, pp. 263–271, Aug. 1997, doi: 10.1016/S0144-8617(97)00037-4.

[24] D. Zhou, Z. Ma, X. Yin, X. Hu, and J. I. Boye, “Structural characteristics and physicochemical properties of field pea starch modified by physical, enzymatic, and acid treatments,” *Food Hydrocoll.*, vol. 93, pp. 386–394, Aug. 2019, doi: 10.1016/J.FOODHYD.2019.02.048.

[25] O. León *et al.*, “Hydrogels based on oxidized starches from different botanical sources for release of fertilizers,” *Int. J. Biol. Macromol.*, vol. 136, pp. 813–

822, Sep. 2019, doi: 10.1016/J.IJBIOMAC.2019.06.131.

[26] S. S. Kolluru, S. Agarwal, S. Sireesha, I. Sreedhar, and S. R. Kale, “Heavy metal removal from wastewater using nanomaterials-process and engineering aspects,” *Process Saf. Environ. Prot.*, vol. 150, pp. 323–355, Jun. 2021, doi: 10.1016/J.PSEP.2021.04.025.

[27] Z. Hu, L. Cai, J. Liang, X. Guo, W. Li, and Z. Huang, “Green synthesis of expanded graphite/layered double hydroxides nanocomposites and their application in adsorption removal of Cr(VI) from aqueous solution,” *J. Clean. Prod.*, vol. 209, pp. 1216–1227, Feb. 2019, doi: 10.1016/J.JCLEPRO.2018.10.295.

[28] A. T. Hoang *et al.*, “Heavy metal removal by biomass-derived carbon nanotubes as a greener environmental remediation: A comprehensive review,” *Chemosphere*, vol. 287, p. 131959, Jan. 2022, doi: 10.1016/J.CHEMOSPHERE.2021.131959.

[29] L. Cossarutto, T. Zimny, J. Kaczmarczyk, T. Siemieniewska, J. Bimer, and J. V. Weber, “Transport and sorption of water vapour in activated carbons,” *Carbon N. Y.*, vol. 39, no. 15, pp. 2339–2346, Dec. 2001, doi: 10.1016/S0008-6223(01)00065-3.

[30] G. Xiao *et al.*, “Superior adsorption performance of graphitic carbon nitride nanosheets for both cationic and anionic heavy metals from wastewater,” *Chinese J. Chem. Eng.*, vol. 27, no. 2, pp. 305–313, Feb. 2019, doi: 10.1016/J.CJCHE.2018.09.028.

[31] R. Shahrokhi-Shahraki, C. Benally, M. G. El-Din, and J. Park, “High efficiency removal of heavy metals using tire-derived activated carbon vs commercial activated carbon: Insights into the adsorption mechanisms,” *Chemosphere*, vol. 264, p. 128455, Feb. 2021, doi: 10.1016/J.CHEMOSPHERE.2020.128455.

[32] C. Lu and H. Chiu, “Adsorption of zinc(II) from water with purified carbon nanotubes,” *Chem. Eng. Sci.*, vol. 61, no. 4, pp. 1138–1145, Feb. 2006, doi: 10.1016/J.CES.2005.08.007.

[33] N. Iwashita, C. R. Park, H. Fujimoto, M. Shiraishi, and M. Inagaki, “Specification for a standard procedure of X-ray diffraction measurements on carbon materials,” *Carbon N. Y.*, vol. 42, no. 4, pp. 701–714, Jan. 2004, doi: 10.1016/J.CARBON.2004.02.008.

[34] T. Xing *et al.*, “Disorder in ball-milled graphite revealed by Raman spectroscopy,” *Carbon N. Y.*, vol. 57, pp. 515–519, Jun. 2013, doi: 10.1016/J.CARBON.2013.02.029.

[35] J. P. Vareda, A. J. M. Valente, and L. Durães, “Assessment of heavy metal pollution from anthropogenic activities and remediation strategies: A review,” *J. Environ. Manage.*, vol. 246, pp. 101–118, Sep. 2019, doi: 10.1016/J.JENVMAN.2019.05.126.

[36] H. A. Hegazi, “Removal of heavy metals from wastewater using agricultural and industrial wastes as adsorbents,” *HBRC J.*, vol. 9, no. 3, pp. 276–282, Dec. 2013, doi: 10.1016/J.HBRCJ.2013.08.004.

[37] X. Qiu and S. Hu, “‘Smart’ materials based on cellulose: A review of the

preparations, properties, and applications," *Materials (Basel).*, vol. 6, no. 3, pp. 738–781, 2013, doi: 10.3390/ma6030738.

[38] A. E. Burakov *et al.*, "Adsorption of heavy metals on conventional and nanostructured materials for wastewater treatment purposes: A review," *Ecotoxicol. Environ. Saf.*, vol. 148, pp. 702–712, Feb. 2018, doi: 10.1016/J.ECOENV.2017.11.034.

[39] P. Pal and F. Banat, "Comparison of heavy metal ions removal from industrial lean amine solvent using ion exchange resins and sand coated with chitosan," *J. Nat. Gas Sci. Eng.*, vol. 18, pp. 227–236, May 2014, doi: 10.1016/J.JNGSE.2014.02.015.

[40] M. B. Ahmed, J. L. Zhou, H. H. Ngo, W. Guo, N. S. Thomaidis, and J. Xu, "Progress in the biological and chemical treatment technologies for emerging contaminant removal from wastewater: A critical review," *J. Hazard. Mater.*, vol. 323, pp. 274–298, Feb. 2017, doi: 10.1016/J.JHAZMAT.2016.04.045.

[41] R. Gusain, K. Gupta, P. Joshi, and O. P. Khatri, "Adsorptive removal and photocatalytic degradation of organic pollutants using metal oxides and their composites: A comprehensive review," *Adv. Colloid Interface Sci.*, vol. 272, p. 102009, Oct. 2019, doi: 10.1016/J.CIS.2019.102009.

[42] Y. Hu, H. L. Tsai, and C. L. Huang, "Effect of brookite phase on the anatase–rutile transition in titania nanoparticles," *J. Eur. Ceram. Soc.*, vol. 23, no. 5, pp. 691–696, Apr. 2003, doi: 10.1016/S0955-2219(02)00194-2.

[43] M. Lazzeri, S. Piscanec, F. Mauri, A. C. Ferrari, and J. Robertson, "Phonon

linewidths and electron-phonon coupling in graphite and nanotubes," *Phys. Rev. B - Condens. Matter Mater. Phys.*, vol. 73, no. 15, pp. 1–6, 2006, doi: 10.1103/PhysRevB.73.155426.

Chater 5

Development of Absorbent Using Starch-Graphite Composite Electrode for Removal of Arsenic and Natural Water in Bangdesh

Chapter 5:Development of Absorbent Using Starch-Graphite Composite Electrode for Removal of Arsenic and Real Water in Bangladesh

5.1 Introduction

Arsenic has properties of both metallic and non-metallic elements, which is the most abundant element in the natural environment [1]. Arsenic is also one of the most toxic elements in water resources, small amounts of arsenic can accumulate in the kidney, bladder, and lungs of the human body and cause carcinogens that threaten human health. As a result, arsenic concentrations have been strictly determined to be less than 10 μg/L and 1.5 μg/L in freshwater and seawater by the World Health Organization (WHO), respectively [2-5]. However, there is still much arsenic existence in water in many countries, such as India, China, Australia, and Bangladesh [5]. The first well-known large-scale arsenic poisoning incident has occurred in Bangladesh. In the beginning 1970s, there are around 10 million hand-pumped wells were installed into Ganges alluvial to avoid pathogens through waterborne prevalent in Bangladesh, however, arsenic contamination in those wells was ignored until about 35-77 million people have been chronically exposed to increased concentrations of arsenic through drinking water in 1990s [6]. Even though people are putting effort into reducing and controlling the concentration of arsenic in water resources, it still has an extremely high concentration in the hydrosphere caused the regular concentration has to be limited under concentration in 50 μg/L by Bangladesh own country [7]. Therefore, the removal

of arsenic contaminants from water in Bangladesh is a matter of urgency

Arsenate [As (V)] and arsenite [As (III)] are the two most common formations in water, and these two forms will be transformed reversed with the different pH values of water, of which trivalent arsenic is more harmful to humans than pentavalent arsenic, so removing trivalent arsenic is the priority for water treatment [8-9]. Many studies have been reported on persistent arsenic exposure to drinking water increased mortality rates from chronic diseases in Bangladesh, such as arsenic specific filter membranes using, co-precipitation with ferric chloride, and adsorbents such as activated alumina [10]. Reverse Osmosis (RO) membrane is the most common method in the realistic water treatment for arsenic removal in Bangladesh, but owing to the frequent membrane changes and high cost makes it impossible for most poor Bengalis to use it widely [11-12]. On the other hand, many studies have confirmed that co-precipitation with ferric chloride has great performance for arsenate [As(V)], but since arsenite [As(III)] is more difficult to remove than As(V), it can be rapidly oxidized to As(V) by oxidants such as hypochlorite, permanganate and hydrogen peroxide, and then chemical precipitation phenomenon occurs [13-15]. However, phosphate and silicate concentrations in the groundwater of Bangladesh can significantly reduce the effectiveness of co-precipitation treatment due to phosphate has been reported to enhance the mobility of arsenic (V) in lead arsenate contaminated soils. Silicate has also been tried to reduce the removal of SO_4^{2-}, SeO_3^{2-}, PO_4^{3-}, and CrO_4^{2-} by iron hydroxide thereby increasing the removal of arsenic [14]. Moreover, adsorbent utilization has also been wildly studied for arsenic compounds removal, aluminum is one of the most popular materials

because of the large surface property, strong reducibility, abundant storage, and low prices, but it has been reported that aluminum readily oxidized when exposed to the liquid phase, forming a dense oxide layer, which weakens its reducing reaction [16-18]. Those conventional methods of arsenic removal have been proven to be effective, most of the techniques have not been utilized on a large scale because of the time-consuming, scarce, and costly materials [18-19]. Therefore, a new method with low cost and high efficiency for arsenic removal is required for helping people who is suffering from arsenic poisoning in Bangladesh.

Absorbent method for water contaminated removal have been already introduced for several decades because of the high benefits, such as large surface, readily Absorbent methods for water contaminated removal have been already introduced for several decades because of the specific sorption function group, large surface, readily discovered in nature, less environmental burden, and low cost [20-23]. Polysaccharides like cellulose, alginate, pectin, and chitosan have been studied for organic and inorganic removal of water treatment [24]. Chitosan had been proven that it can purify arsenic compounds from groundwater, it has been shown that chitosan has the functional group of amino ($-NH_2$), acetamido ($-CH_2CONH-$), and hydroxyl (-OH) that can effectively absorb arsenic compounds from water [25-27]. However, the pH value has must be controlled in 4-9 [27]. Meanwhile, starch also has shown great efficiency for heavy metal and arsenic removal in water treatment because the hydroxyl (-OH) group is surrounded in the backbone, but due to the surface limitation of the starch, it has not been widely used so far [28]. Here we would like to focus on the absorbent of starch

combined with carbon material to find a quick and high-efficiency method for arsenic removal.

Carbon material has also been found that it can be used as an absorbent for arsenic compound treatment from water. Carbon felt immobilized with butyl rubber exhibited nearly 60 μmol of arsenic can be absorbed in 50 minutes at 0.4 V potential charged but after 60 minutes the absorption efficiency became into saturation due to the surface of carbon felt stained with arsenic and other heavy metal compounds [29]. Thus, expanding the surface area is a big challenge for carbon material utilization. We would like to pay attention to porous graphite. Graphite has high electrical conductivity with a combination of Sp^2 and Sp^3, and has a multilayer porous surface that can dope another absorbent inside and lead much amount of arsenic can be absorbed compared to carbon felt with other bio-absorbent on the surface [30].

In this study, we applied the new absorbent at different voltages on only arsenic removal and mixed several heavy metals with arsenic. Moreover, the real water samples from the Padama River, wells, and tap water from Bangladesh were analyzed, and the contaminates removal experiments were conducted from real water samples as well. This study is expected to be effective in adsorbing both arsenic and other contaminants from inside the water and could provide a potential new adsorbent material.

5.2 Experimentals

5.2.1 Chemicals and Materials

Soluble starch and potassium chloride were purchased from Fujifilm Wako

Chemicals, respectively. Heavy metal (Pb, Cu, Ni, Al, Cd) and arsenic standard solution were purchased from Kanto Chemical Co., Inc. which are reagent grade. Concentrated Sulfuric acid was added to the real water sample for guaranteeing water quality, which was purchased from Fujifilm Wako Chemicals. Graphite carbon plates were donated by Hitachi Chemical Co., Ltd. Starch doped graphite carbon plate, graphite carbon plate, Ag/AgCl electrode as working electrode (WE), counter electrode (CE), and reference electrode (RE), respectively. Arsenic pack test kits were used to test real water in Bangladesh, which were purchased from Kyoritsu Chemical-Check Lab Co., Ltd.

5.2.2 Instruments

The carbon plates were analyzed by using Raman spectrometer (JASCO, RMP 500) and X-Ray Diffraction (XRD, Rigaku SmartLab) for detecting its bond strengths and constitution, here carbon plate samples were grounded into powder type. Scanning electrode microscopy (SEM, Hitachi, S4800 series) was used to observe the porous size of carbon plates and Molecular Force Probe 3D (MFP-3D, Sylum Research, MFP-3D-SA) was applied to detect the surface change of graphite porous carbon plate before and after doping starch. Inductively Coupled Plasma Spectroscopy (ICP, Shimazu Corporation, ICPE9000) was conducted to analyze heavy metals and arsenic concentration from water samples before and after treatment. Ultra Visible spectrophotometer (UV, Hitachi, U3000) was applied for detecting the arsenic concentration from the pack test in Bangladesh. The combination process for the new absorbent vacuumed system, and an oven at 80°C was used for drying new adsorbent materials. The arsenic and heavy metals absorption was conducted using an Electrochemical Instrument (Ho-kuto Denko, HZ-7000)

5.2.3 Synthesis of absorbents

Soluble starch powder of 1 g, 2 g, 4 g, 8 g, 10 g was weighed and dissolved into 100ml Mili-Q water and stirred until all particles had become homogeneous, respectively. Carbon plats were cut into different area sizes and weighed beforehand immersed in the starch solution individually. Subsequently, the vacuum system has been applied for doping the starch into carbon plates for 120 min at the 150 L/min ultimate pressure. The weights of carbon plates were measured again after 80°C oven-dried.

5.2.4 Absorption experiments with sorbents

The absorption experiments were carried out in Bangladesh locally and in the laboratory, respectively. The experiments were mainly divided into those for the absorption of only arsenic standard solutions and those for the mixture of heavy metals with arsenic standard solutions for 120 min absorption processes. The standard solution for arsenic and heavy metals was prepared from 250 mg/L to 10 mg/L. The real sources of water samples were obtained from the middle part of the Padama River, wells, and tap water in Rajshahi City, which is located in the northwest part of Bangladesh. And the test real water experiments have analyzed the compounds of contaminants and carried out the absorption subsequently. And the standard solution and real water samples were conducted at the different potentials application (-0.5 v to 0.5 V).

5.3 Results

5.3.1 Characterization of absorbents

In this study, two kinds of graphite porous carbon plates were prepared as potential materials. XRD was used to detect the component of two porous carbon plates using Cu-Ka radiation of 1.5405Å wavelength and a scanning speed of 2° min^{-1}. Two types of porous carbon showed the peak of XRD patterns at 2θ = 26.7° where are located at the typical graphite peak [31] in Figure 1 (a), (b) shown. Moreover, in Figure 1. (b) was found that at 2θ values of 47.6°, 53.5°, and 55.1°; and 2θ values peak of rutile were found at 35.6° and 61.0°, which is coincided with crystal planes of anatase (200), (105), and (211); rutile crystal planes of (101) and (310) [32]. As a result, Figure 1. (b) graphite porous carbon plate shows a hydrophilic property. Raman spectra of two types of porous carbon plates were exhibited in Figure 1 (a), (b) to detect the species of carbon crystallization. As a result, the main peaks were exhibited at 1582 cm^{-1} and 1350 cm^{-1}, respectively. The Raman peak around 1582 cm^{-1} is a typical Raman peak of bulk crystalline graphite, called the G-band. This peak is the basic vibration mode of graphite crystals. The intensity is related to the size of the crystal [33]. 1350 cm^{-1} peak value is derived from the vibration of the crystalline carbon edge of the graphite, called D-band. Regarding the Raman spectra, graphite material is dominating two kinds of porous carbon because the high G-band value was exposed. In addition, the high value of the G-band and D-band ratio represents good electroconductivity property [34]. The ratio of G-band and D-band of two carbon electrodes are 0.45 and 0.48, respectively,

approximately at the same values of the ratio. Whereas, Figure (b) shows the hydrophilic property, which has much potential as absorbents considering the experiments were conducted at the liquid phase. SEM images in Figure 1. (c), (d) showed the pore size of two types of graphite porous carbon plate, the cavity of the pore was measured in 5 μm regarding controlled in magnification: 4000, working distance: 17.4 mm, acceleration voltage: 5KV, and emission current: 10 μA condition. According to the SEM images results, two types of graphite porous carbon plate exposed a similar size of pore size, and the multi-layer sheets were expressed as well. Two types of graphite carbon plate could be a potential material.

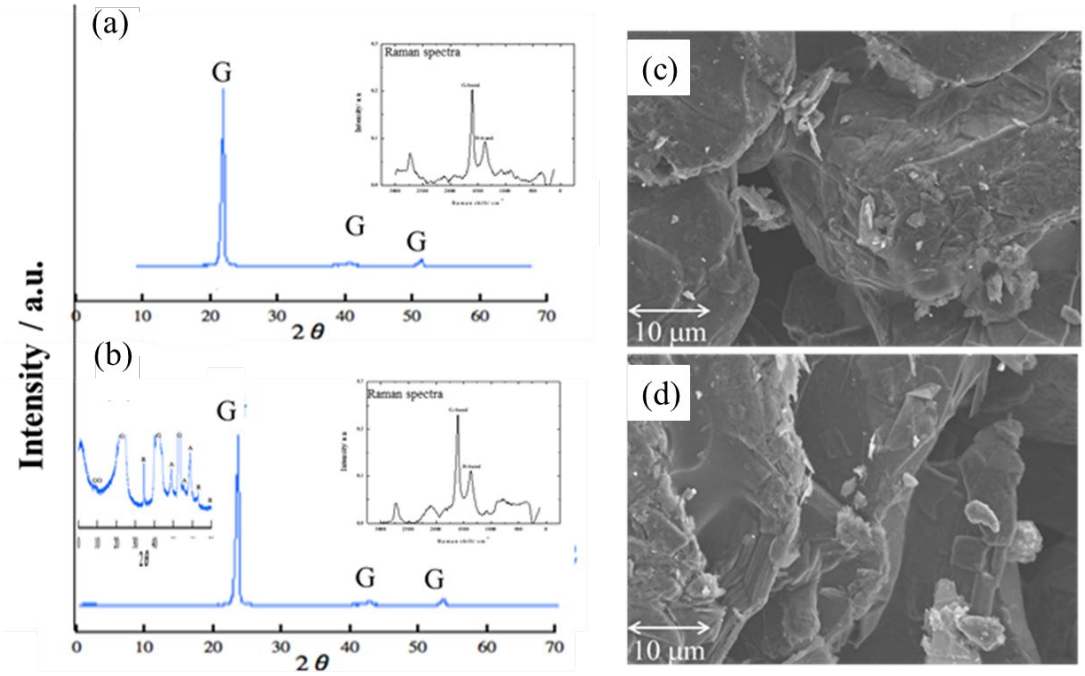

Figure 1. X-ray diffraction and Raman spectra of (a) Porous carbon; (b) TiO_2 doped graphite porous carbon; SEM imagines of (c) Porous carbon; (d) TiO_2 doped graphite porous carbon. (I: 10 mA V:5 kV Mag: 4000 WD: 17.4 mm)

5.3.2 Absorbent composition

The soluble starch solutions were prepared by different concentrations (1%, 2%, 4%, 8%, 10%) for doping into the porous carbon plates (1 cm × 1 cm × 0.2 cm) in 120 mins by a vacuum system. As a result, bulk graphite porous carbon showed no weight change before and after doping, the titanium added type of graphite showed 0.1g weight increased after 120 min doping process in 10% starch solution. Thus, in this research, we would like to choose 10% starch as the doping standard solution and the titanium added graphite porous carbon as one part of the new absorbent.

In order to know the proper graphite porous carbon plate area selection, carbon plates are also cut into different sizes, and Figure 2 shows the relationship between the size of the carbon plate area and the increase in starch weight.

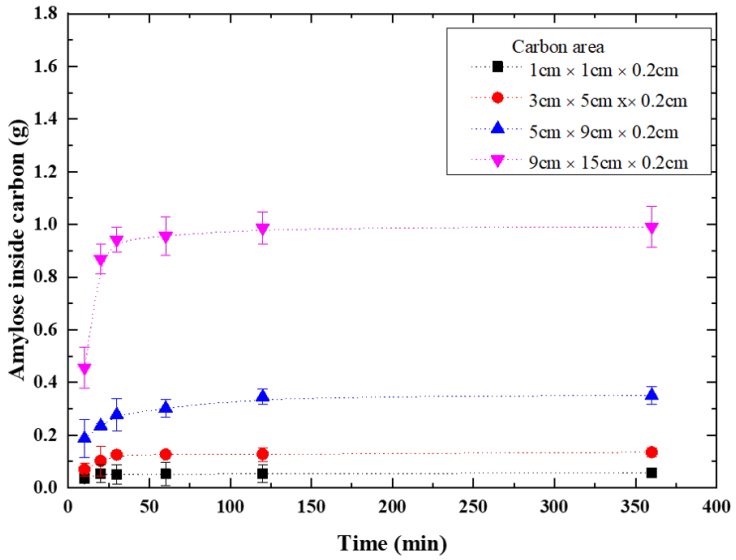

Figure 2. Time dependence of amylose forcing doped into TiO2 doped graphite porous carbon.

When the carbon plate area is tripled, the starch weight is correspondingly tripled, thus,

there is a proportional incremental relationship between carbon area and starch amount inside. And for considering the electrochemical method was conducted in a laboratory, the area of carbon plate was chosen the 5.0 cm x 9.0 cm x 0.2cm due to easier operation.

5.3.3 Water sampling, rice sampling, and analysis

Water samplings were conducted in Rajshahi City, which is located in the northwest part of Bangladesh. Three types of water samples were obtained, river samples from the Padama River, tap water from the local household, and the water of the well (groundwater) in Rajshahi University. Figure 3 showed the location of river water sampling, three sampling spots were spaced 20 km apart on average from the Padama River, and the depth of tapwater and wells are 50 m and 20 m according to interview local people, respectively.

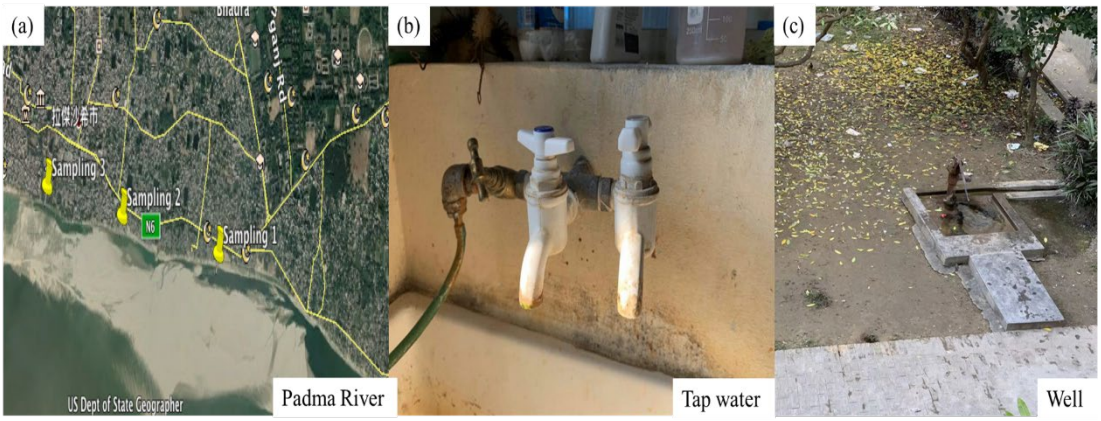

Figure 3. Water sampling location in Bangladesh.

The real water samples were analyzed by arsenic pack test kit in Bangladesh immediately and ICP in Japan. Table 1 showed the results of water samples after ICP was analyzed. There are other heavy metals and high phosphate contaminants in three water types and all of the concentrations of elements are exceeding the regulation from

WHO.

Table 1. The contaminants in real water samples.

	As (mg/L)	Al (mg/L)	Cd (mg/L)	Cu (mg/L)	Ni (mg/L)	Pb (mg/L)	P (mg/L)
River sample	2.3	4.5	0.3	0.5	0.3	2.8	2.7
Tap water	5.2	8.4	0.2	0.3	0.4	2.9	3.1
Well (Groundwater)	3.1	3.3	0.1	0.3	0.2	2.1	4.9

In table 1 showed the results of river samples are average values owing to the three locations are exhibited similar results. Arsenic concentration in the river showed the lowest concentration, whereas, tap water exhibited the highest concentration even people are using the water for drinking and cooking. According to the results, the arsenic formation may be formed with the phosphate and showed the As(III) and As(V) simultaneously. Moreover, other heavy metals showed the exceeded regulation level as well. All of those toxic elements are necessary to be considered.

Due to the water samples contaminated with arsenic, cooking rice is considered to be tested due to the water transformation. As well known, starch is readily extracted from the cooking rice and sticky rice, and if the starch has the potential for absorbing arsenic, the cooking rice may contain arsenic as well. We brought six kinds of cooking polished rice from the local market in Bangldesh and extracted the starch solid to test the arsenic concentration inside. Figure 4 showed the arsenic concentration from the six kinds of cooking rice. The species of rice could not identify due to the local people having less agricultural knowledge and also people do not pay attention to the rice

species in Bangladesh.

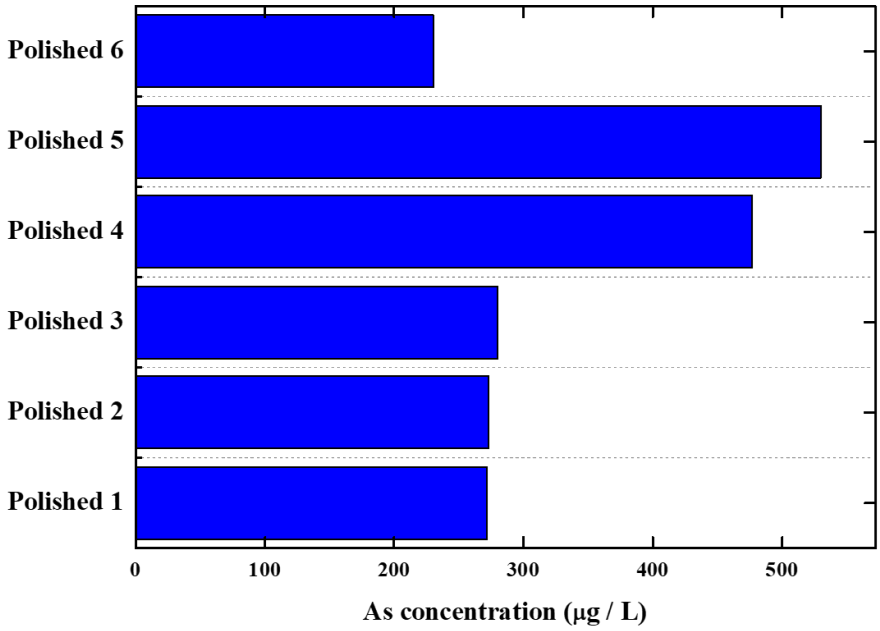

Figure 4. The arsenic concentration in local cooking rice of Bangladesh.

Figure 4 illustrated that the polished 4 and 5 contained a high concentration of arsenic among those sis cooking rice species. We interviewed the local people of the plantation, the rice ower answered that only these two species of rice were planted far away from the Padma River, people is using the well water for irrigation instead of using river water. Regarding the interview and table 1, the water from wells is contaminated by high arsenic caused the rice was contaminated as well through the water irrigation. Therefore, it is necessary to remove arsenic and other heavy metals from water to protect agricultural safety.

5.3.4 Bulk Arsenic and mixed heavy metals absorption in standard solution

In this study, bulk arsenic absorption experiments were conducted to detect the critical given potential. As previously mentioned, 0.3g of starch and titanium added graphite porous carbon plate was applied as potential absorbents. In the last chapter, we already discussed amylose with graphite could absorb cations from water and had a great efficiency of absorption when the WE electrode was be charged at -0.5 V potential. Thus, we assumed that the starch with titanium added graphite porous carbon plate as WE electrode at -0.5 V applied could absorb arsenic as well. Figure 5 showed the results for bulk arsenic absorption at a given -0.5 V potential. The initial concentrations of arsenic were prepared from 10 mg/L to 250 mg/L for 120 mins absorption process. The maximum absorption amount was approximately 95.341 mg/L.

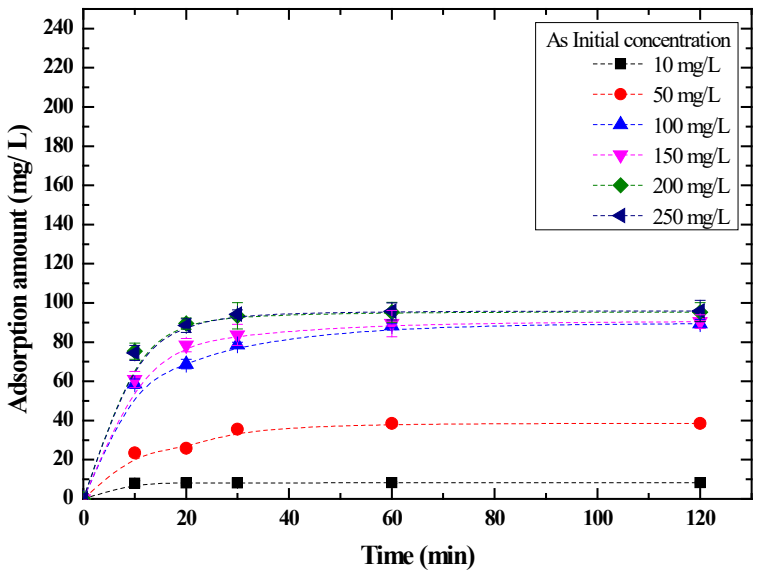

Figure 5. The absorption amount of bulk arsenic compounds at -0.5 V using 0.3 g starch added into the titanium with graphite porous carbon plate.

The absorption rate was optimal at the first 30 min, but the initial arsenic concentration exceeded 200 mg/L, the rate slowed down and saturation gradually occurred. Thus, it is known that the maximum adsorption capacity of arsenic can reach less than 100 mg/L at a fixed electrode area and given voltage. This phenomenon could be considered that as the electrostatic reaction accelerates the rate of mobility of arsenic ions in water at the first 30 mins, more arsenic ions are absorbed on the surface of the absorbent, resulting in left arsenic elements in water could not able to through the absorption material, even if the absorption process is consumed. Therefore, we considered changing the potential applied. Figure 6 showed the different potential given from -1.0 v to +1.0 V at the initial As concentration at 200 mg/L. It was found that the potential

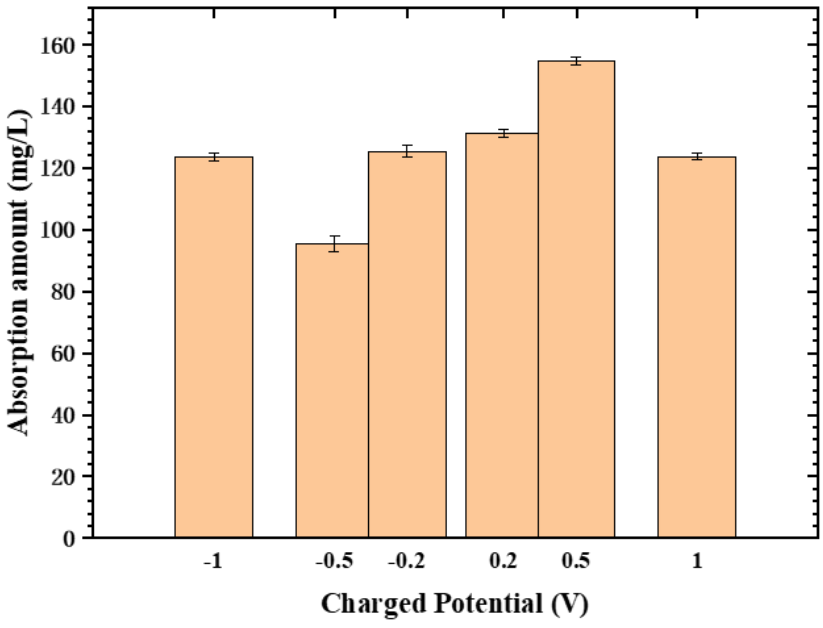

Figure 6. Effect of voltage change on arsenic absorption amount at 200 mg/L initial concentration using 0.3 g starch added into the titanium with graphite porous carbon plate.

at +0.5 V showed a perfect performance although the absorption rate is slow at the essential 30 min, the process continues after 60 min and the absorption amount was over 100 mg/L in 120 min. As a result, the optimized potential for bulk arsenic absorption would be at +0.5 V.

On the other hand, the analysis of water samples showed that heavy metals and arsenic are present at the same time, so the simultaneous removal of elemental arsenic and heavy metals experiments were also explored. In the previous chapter, it has been concluded that heavy metals can wait for good absorption at -0.5 V, so considering simultaneous absorption is requested, we introduced starch into the WE and the CE, and first applied a voltage of -0.5 V to the WE for adsorption for 120 min, and then converted the WE to the CE to increase the voltage of +0.5 V. Figure 7 showed the results for each heavy metal and arsenic absorption in standard solutions. The results showed that heavy metal absorption abilities were determined by the size of the ionic radius order and due to absorption competition occurred, arsenic presented little absorption effect during the absorption at a negative voltage, but at the subsequent 120 min of positive voltage, arsenic absorption reached a much better boost than in the solution of only arsenic ions owing to the increase in the rate of activity of the arsenic ions made in the early stage.

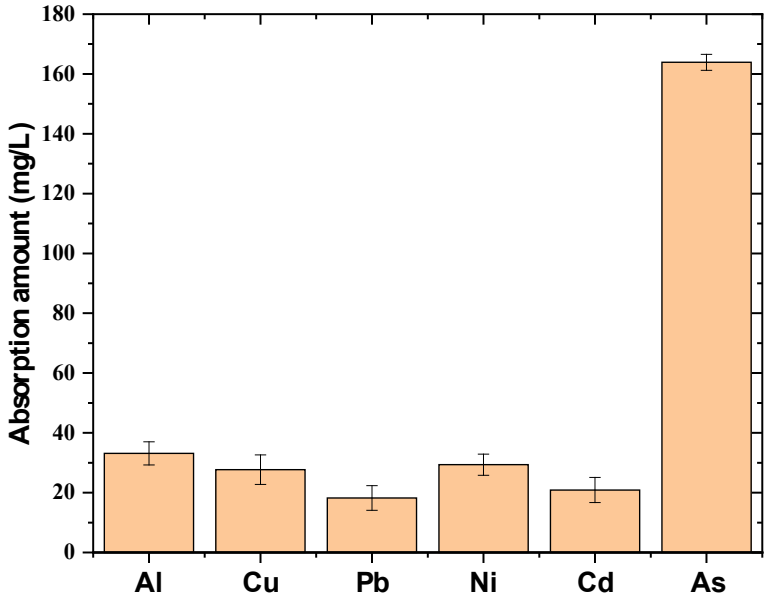

Figure 7. The absorption amount of heavy metal and arsenic mixed standard solution using 0.3 g starch added into the titanium with graphite porous carbon plate for 240 min absorption process.

5.4 Conclusion

In this study, we investigated the toxic compounds in the Padama River where is located in the northwest of Bangladesh, and targeted the sorption of arsenic from raw water onto starch added into the graphite porous carbon plate absorbent. The results showed that several heavy metals were contaminated in raw water, the order of main occupied toxic compound species: Al, Pb, As, Cu, Ni, Cd. Those concentrations levels are beyond the standard regulations by WHO provided. On the other hand, experimental data of removal of arsenic compounds indicated that as a +0.5 V voltage was charged on the absorbent, there is a great performance for decreasing arsenic compounds from

raw water. We believe that this experimental design could apply to the industrial level by increasing the weight of α-amylose and the area of the carbon plate.

5.5 References

[1] X. Meng, G. P. Korfiatis, C. Christodoulatos, and S. Bang, "Treatment of arsenic in Bangladesh well water using a household co-precipitation and filtration system," *Water Res.*, vol. 35, no. 12, pp. 2805–2810, 2001, doi: 10.1016/S0043-1354(01)00007-0.

[2] I. D. Urango-Cárdenas, S. Burgos-Núñez, L. Á. Ospina Herrera, G. Enamorado-Montes, and J. L. Marrugo-Negrete, "Determination of arsenic chemical species in rice grains using high-performance liquid chromatography coupled to hydride generator with atomic fluorescence detector (HPLC-HG-AFS)," *MethodsX*, vol. 8, 2021, doi: 10.1016/j.mex.2021.101281.

[3] M. E. Huq *et al.*, "Arsenic in a groundwater environment in Bangladesh: Occurrence and mobilization," *J. Environ. Manage.*, vol. 262, no. January 2019, p. 110318, 2020, doi: 10.1016/j.jenvman.2020.110318.

[4] N. Sohel *et al.*, "Arsenic in drinking water and adult mortality: A population-based cohort study in rural Bangladesh," *Epidemiology*, vol. 20, no. 6, pp. 824–830, 2009, doi: 10.1097/EDE.0b013e3181bb56ec.

[5] M. Argos *et al.*, "Arsenic exposure from drinking water, and all-cause and chronic-disease mortalities in Bangladesh (HEALS): A prospective cohort study," *Lancet*, vol. 376, no. 9737, pp. 252–258, 2010, doi: 10.1016/S0140-

6736(10)60481-3.

[6] A. A. Meharg and M. Rahman, “Arsenic contamination of Bangladesh paddy field soils: Implications for rice contribution to arsenic consumption,” *Environ. Sci. Technol.*, vol. 37, no. 2, pp. 229–234, 2003, doi: 10.1021/es0259842.

[7] P. L. Smedley and D. G. Kinniburgh, “A review of the source, behaviour and distribution of arsenic in natural waters,” *Appl. Geochemistry*, vol. 17, no. 5, pp. 517–568, 2002, doi: 10.1016/S0883-2927(02)00018-5.

[8] M. Banerjee *et al.*, “High arsenic in rice is associated with elevated genotoxic effects in humans,” *Sci. Rep.*, vol. 3, pp. 1–8, 2013, doi: 10.1038/srep02195.

[9] M. O. Arnous and M. A. A. Hassan, “Heavy metals risk assessment in water and bottom sediments of the eastern part of Lake Manzala, Egypt, based on remote sensing and GIS,” *Arab. J. Geosci.*, vol. 8, no. 10, pp. 7899–7918, 2015, doi: 10.1007/s12517-014-1763-6.

[10] E. Byeon, H.-M. Kang, C. Yoon, and J.-S. Lee, “Toxicity mechanisms of arsenic compounds in aquatic organisms,” *Aquat. Toxicol.*, vol. 237, no. May, p. 105901, 2021, doi: 10.1016/j.aquatox.2021.105901.

[11] M. Azizur Rahman and H. Hasegawa, “Arsenic in freshwater systems: Influence of eutrophication on occurrence, distribution, speciation, and bioaccumulation,” *Appl. Geochemistry*, vol. 27, no. 1, pp. 304–314, 2012, doi: 10.1016/j.apgeochem.2011.09.020.

[12] Y. M. Zheng, S. W. Zou, K. G. N. Nanayakkara, T. Matsuura, and J. P. Chen, “Adsorptive removal of arsenic from aqueous solution by a PVDF/zirconia

blend flat sheet membrane," *J. Memb. Sci.*, vol. 374, no. 1–2, pp. 1–11, 2011, doi: 10.1016/j.memsci.2011.02.034.

[13] A. Abejón, A. Garea, and A. Irabien, "Arsenic removal from drinking water by reverse osmosis: Minimization of costs and energy consumption," *Sep. Purif. Technol.*, vol. 144, pp. 46–53, 2015, doi: 10.1016/j.seppur.2015.02.017.

[14] F. Battaglia-Brunet, C. Crouzet, A. Burnol, S. Coulon, D. Morin, and C. Joulian, "Precipitation of arsenic sulphide from acidic water in a fixed-film bioreactor," *Water Res.*, vol. 46, no. 12, pp. 3923–3933, 2012, doi: 10.1016/j.watres.2012.04.035.

[15] A. B. M. R. Islam, J. P. Maity, J. Bundschuh, C. Y. Chen, B. K. Bhowmik, and K. Tazaki, "Arsenic mineral dissolution and possible mobilization in mineral-microbe-groundwater environment," *J. Hazard. Mater.*, vol. 262, pp. 989–996, 2013, doi: 10.1016/j.jhazmat.2012.07.022.

[16] M. Bissen, M. M. Vieillard-Baron, A. J. Schindelin, and F. H. Frimmel, "TiO2-catalyzed photooxidation of arsenite to arsenate in aqueous samples," *Chemosphere*, vol. 44, no. 4, pp. 751–757, 2001, doi: 10.1016/S0045-6535(00)00489-6.

[17] C. M. Babu *et al.*, "Characterization of reduced graphene oxide supported mesoporous Fe2O3/TiO2 nanoparticles and adsorption of As(III) and As(V) from potable water," *J. Taiwan Inst. Chem. Eng.*, vol. 62, pp. 199–208, 2016, doi: 10.1016/j.jtice.2016.02.005.

[18] I. Ali and V. K. Gupta, "Advances in water treatment by adsorption

technology," *Nat. Protoc.*, vol. 1, no. 6, pp. 2661–2667, 2007, doi: 10.1038/nprot.2006.370.

[19] L. Beesley and M. Marmiroli, "The immobilisation and retention of soluble arsenic, cadmium and zinc by biochar," *Environ. Pollut.*, vol. 159, no. 2, pp. 474–480, 2011, doi: 10.1016/j.envpol.2010.10.016.

[20] R. Amen *et al.*, "A critical review on arsenic removal from water using biochar-based sorbents: The significance of modification and redox reactions," *Chem. Eng. J.*, vol. 396, no. April, 2020, doi: 10.1016/j.cej.2020.125195.

[21] H. Li, X. Dong, E. B. da Silva, L. M. de Oliveira, Y. Chen, and L. Q. Ma, "Mechanisms of metal sorption by biochars: Biochar characteristics and modifications," *Chemosphere*, vol. 178, pp. 466–478, 2017, doi: 10.1016/j.chemosphere.2017.03.072.

[22] B. Zhi *et al.*, "Ordered mesoporous MnO2 as a synergetic adsorbent for effective arsenic(iii) removal," *J. Mater. Chem. A*, vol. 2, no. 7, pp. 2374–2382, 2014, doi: 10.1039/c3ta13790b.

[23] N. Aramesh, A. R. Bagheri, and M. Bilal, "Chitosan-based hybrid materials for adsorptive removal of dyes and underlying interaction mechanisms," *Int. J. Biol. Macromol.*, vol. 183, pp. 399–422, 2021, doi: 10.1016/j.ijbiomac.2021.04.158.

[24] Q. Xue, Y. Ran, Y. Tan, C. L. Peacock, and H. Du, "Arsenite and arsenate binding to ferrihydrite organo-mineral coprecipitate: Implications for arsenic mobility and fate in natural environments," *Chemosphere*, vol. 224, pp. 103–

110, 2019, doi: 10.1016/j.chemosphere.2019.02.118.

[25] A. Choodari Gharehpapagh, M. R. Farahpour, and S. Jafarirad, “The biological synthesis of gold/perlite nanocomposite using Urtica dioica extract and its chitosan-capped derivative for healing wounds infected with methicillin-resistant Staphylococcus aureus,” *Int. J. Biol. Macromol.*, vol. 183, pp. 447–456, 2021, doi: 10.1016/j.ijbiomac.2021.04.150.

[26] S. Ansari, N. Sami, D. Yasin, N. Ahmad, and T. Fatma, “Biomedical applications of environmental friendly poly-hydroxyalkanoates,” *Int. J. Biol. Macromol.*, vol. 183, pp. 549–563, 2021, doi: 10.1016/j.ijbiomac.2021.04.171.

[27] Y. M. Li, R. fang Zhong, J. Chen, and Z. G. Luo, “Structural characterization, anticancer, hypoglycemia and immune activities of polysaccharides from Russula virescens,” *Int. J. Biol. Macromol.*, vol. 184, no. June, pp. 380–392, 2021, doi: 10.1016/j.ijbiomac.2021.06.026.

[28] M. Nasrollahzadeh, M. Sajjadi, S. Iravani, and R. S. Varma, “Starch, cellulose, pectin, gum, alginate, chitin and chitosan derived (nano)materials for sustainable water treatment: A review,” *Carbohydr. Polym.*, vol. 251, no. August 2020, p. 116986, 2021, doi: 10.1016/j.carbpol.2020.116986.

[29] L. Wang *et al.*, “Effects of anode/cathode electroactive microorganisms on arsenic removal with organic/inorganic carbon supplied,” *Sci. Total Environ.*, vol. 798, p. 149356, 2021, doi: 10.1016/j.scitotenv.2021.149356.

[30] A. Islam *et al.*, “Novel micro-structured carbon-based adsorbents for notorious arsenic removal from wastewater,” *Chemosphere*, vol. 272, p. 129653, 2021,

doi: 10.1016/j.chemosphere.2021.129653.

[31] J. Światowska, V. Lair, C. Pereira-Nabais, G. Cote, P. Marcus, and A. Chagnes, “XPS, XRD and SEM characterization of a thin ceria layer deposited onto graphite electrode for application in lithium-ion batteries,” *Appl. Surf. Sci.*, vol. 257, no. 21, pp. 9110–9119, 2011, doi: 10.1016/j.apsusc.2011.05.108.

[32] G. qing Liu, X. jun Pan, J. Li, C. Li, and C. lu Ji, “Facile preparation and characterization of anatase TiO2/nanocellulose composite for photocatalytic degradation of methyl orange,” *J. Saudi Chem. Soc.*, vol. 25, no. 12, p. 101383, 2021, doi: 10.1016/j.jscs.2021.101383.

[33] K. Li, Q. Liu, H. Cheng, M. Hu, and S. Zhang, “Classification and carbon structural transformation from anthracite to natural coaly graphite by XRD, Raman spectroscopy, and HRTEM,” *Spectrochim. Acta - Part A Mol. Biomol. Spectrosc.*, vol. 249, p. 119286, 2021, doi: 10.1016/j.saa.2020.119286.

[34] D. Kot *et al.*, “Porous graphite as stationary phase for the chromatographic separation of polymer additives - determination of adsorption capability by Raman spectroscopy and physisorption,” *J. Chromatogr. A*, vol. 1625, p. 461302, 2020, doi: 10.1016/j.chroma.2020.461302.

Chapter 6

Summary and Conclusions

Chapter 6 : Summary and Conclusions

Alginate is known as a good adsorbent of radioactive substance, such as Sr^{2+}. However, due to the presence of substances other than Sr^{2+} in water, the Sr^{2+} adsorption capacity of alginate decreases as preexistence material.

In this study, alginate solution was doped into the TiO_2 vacuum impregnated porous carbon electrode to amplify the capacity of Sr^{2+} sorption. The alginate doped TiO_2 porous carbon electrode adsorbents performance depends on the initial Sr^{2+} concentration. In solutions containing strontium only, alginate doped TiO_2 porous carbon electrode adsorbents contained 50 μmol/ L of alginate exhibits the best performance. Whereas, in solutions is containing complex mixture require more amount of alginate due to the competition of other ions. Compared with alginate sorption method and alginate doped TiO_2 porous carbon electrode method of sorption of strontium, and for removing strontium nearby disaster of Fukushima seawater, alginate doped TiO_2 porous carbon electrode used are the best choices.

The structure of amylose shows many hydroxyl groups surrounded by the bond, which is easy to catch the cations of heavy metals in water. However, due to current heavy metals contamination in water are kinds of variety, α- amylose shows a limited capacity. In this study, for removing heavy metals, 6 pieces of 2920 μmol/ L amylose concentration with 1 cm × 1 cm TiO_2 doped porous carbon show the best performance in the heavy metal mixed solution. A total of 20 mg/L of toxic heavy metal ions were absorbed in 30 minutes. The composited absorbent of amylose/ TiO_2 doped porous

carbon with applying a potential increased amylose sorption capacity and efficiency.

Furthermore, in this study, experiments on arsenic adsorption were also conducted regarding the absorption efficiency of heavy metals, and real water samples from Bangladesh were tested in practice. By analyzing the water samples of Bangladesh, there are a lot of toxic heavy metals in the drinking water in addition to a large number of arsenic compounds, resulting in a large number of toxic substances in the grain rice as well. Through the absorption results of heavy metals in Chapter 4 described, the composite absorption materials were used as WE and CE in simultaneous, and the absorption efficiency of arsenic elements was increased by applying positive and negative charge interconversion, and a certain amount of heavy metals could be absorbed at the same time.

Therefore, in this research, the new synthetic absorbent materials exhibit both adsorption of radioactive materials, heavy metals, and elemental arsenic, and because the absorbent materials do not have a desorption effect, secondary treatment and environmental burden can be reduced. Moreover, the basic absorbent materials used are abundant in nature and inexpensive. I believe that the new composite adsorbent material developed by myself can be used in real life as a potential and efficient adsorbent material in the future.